NASA Technical Memorandum 107494

A General Reversible Hereditary Constitutive Model: Part I—Theoretical Developments

A.F. Saleeb
University of Akron, Akron, Ohio

S.M. Arnold
Lewis Research Center, Cleveland, Ohio

National Aeronautics and
Space Administration

Lewis Research Center

December 1997

Available from

NASA Center for Aerospace Information
800 Elkridge Landing Road
Linthicum Heights, MD 21090-2934
Price Code: A03

National Technical Information Service
5287 Port Royal Road
Springfield, VA 22100
Price Code: A03

A General Reversible Hereditary Constitutive Model : Part I Theoretical Developments

A. F. Saleeb*
Department Civil Engineering
University of Akron
Akron, OH 44325

S. M. Arnold
National Aeronautics and Space Administration
Lewis Research Center
Cleveland OH, 44135

Abstract

Using an internal-variable formalism as a starting point, we describe the viscoelastic extension of a previously-developed viscoplasticity formulation of the complete potential structure type. It is mainly motivated by experimental evidence for the presence of rate/time effects in the so-called quasilinear, reversible, material response range. Several possible generalizations are described, in the general format of hereditary-integral representations for non-equilibrium, stress-type, state variables, both for isotropic as well as anisotropic materials. In particular, thorough discussions are given on the important issues of thermodynamic admissibility requirements for such general descriptions, resulting in a set of explicit mathematical constraints on the associated kernel (relaxation and creep compliance) functions. In addition, a number of explicit, integrated forms are derived, under stress and strain control to facilitate the parametric and qualitative response characteristic studies reported here, as well as to help identify critical factors in the actual experimental characterizations from test data that will be reported in Part II.

Keywords: viscoelasticity, hereditary behavior, **TIMETAL 21S**, nonisothermal, deformation, multiaxial, thermodynamics

*Research funded by NASA Lewis under Grant NAG3-1747

1 Introduction

A number of advanced material systems (for example metallic, polymer and ceramic based systems) are currently being researched and evaluated for high temperature air frame and propulsion system applications. As a result, numerous computational methodologies for predicting both deformation and life for these classes of materials are under development. An integral part of these methodologies is an accurate and computationally efficient constitutive model for the matrix constituent in such systems. Furthermore, because of the proposed elevated operation temperatures for which these systems are designed, the required constitutive models must account for both time-dependent and time-independent deformations. For example considering that most aerospace engine designs are typically limited to the quasilinear stress and strain regimes, the reversible time-dependent response component becomes dominate in comparison to the irreversible component. Alternatively, one can envision another extreme case (e.g., in polymer and rubber based systems under varying temperatures) in which a purely reversible viscous response is present. And lastly, an obvious natural extension for general applicability is the middle ground in which a combined reversible and irreversible representation is required.

To accomplish this we will **extend** a previously developed, complete potential based, framework [1],[2] utilizing internal state variables [[3],[4]] which was put forth for the derivation of **time-independent** reversible and time-dependent irreversible constitutive equations. This framework, and consequently the resulting constitutive model, is termed complete because the existence of the total (integrated) form of the Gibb's complementary free energy and complementary dissipation potentials are assumed **a priori**. In outline form, expressions for the Gibb's thermodynamic and the complementary dissipation potential functions are assumed in terms of a number of state and internal variables characterizing the changing internal structure of the material. For instance given the Gibb's potential in the following form

$$\Phi = \Phi(\sigma_{ij}, \alpha_\gamma, T, \epsilon^I_{ij}) \tag{1}$$

and assuming **a priori** that the inelastic strain is an **independent parameter** (and not an internal state variable), for example

$$\Phi = \bar{E}(\sigma_{ij}, T) - \sigma_{ij}\epsilon^I_{ij} + \bar{H}\,(\alpha_\gamma, T) - \frac{\sigma_{kk}}{3}\omega(T - T_o), \tag{2}$$

an expression for the total strain rate can be obtained by differentiating, that is,

$$\dot{e}_{ij} = \frac{d}{dt}\left(\frac{-\partial\Phi}{\partial\sigma_{ij}}\right) = C_{ijrs}\dot{\sigma}_{rs} + \dot{\epsilon}^I_{ij} + \left[\frac{-\partial^2\bar{E}(\sigma_{ij})}{\partial\sigma_{ij}\partial T} + \frac{\delta_{ij}}{3}\left(\omega + \frac{\partial\omega}{\partial T}\Delta T\right)\right]\dot{T} \tag{3}$$

as well as the rate of change of the conjugate internal variables (A_ξ),

$$\dot{A}_\xi = \frac{d}{dt}\left(\frac{-\partial\Phi}{\partial\alpha_\xi}\right) = Q_{\xi\gamma}\dot{\alpha}_\gamma + \theta_\xi\dot{T} \tag{4}$$

where

$$C_{ijrs} = \frac{-\partial^2 \Phi}{\partial \sigma_{ij} \partial \sigma_{rs}} = \frac{-\partial^2 \bar{E}(\sigma_{ij}, T)}{\partial \sigma_{ij} \partial \sigma_{rs}} \tag{5}$$

and

$$Q_{\xi\gamma} = \frac{-\partial^2 \Phi}{\partial \alpha_\xi \partial \alpha_\gamma} = \frac{-\partial^2 \bar{H}(\alpha_\gamma, T)}{\partial \alpha_\xi \partial \alpha_\gamma} \tag{6}$$

are the external and internal compliance operators, respectively, and

$$\theta_\xi = \frac{-\partial^2 \Phi}{\partial \alpha_\xi \partial T} = \frac{-\partial^2 \bar{H}(\alpha_\gamma, T)}{\partial \alpha_\xi \partial T} \tag{7}$$

is the change in the conjugate internal variable (A_ξ) with temperature. Note the three terms in eqn. (3) may then be identified from left to right as the elastic (time-independent reversible), inelastic (irreversible), and thermal expansion components of the total strain rate, respectively. Thus,

$$\dot{e}_{ij} = \dot{\epsilon}^R_{ij} + \dot{\epsilon}^I_{ij} + \dot{\epsilon}^T_{ij} \tag{8}$$

where

$$\dot{\epsilon}^R_{ij} = C_{ijrs} \dot{\sigma}_{rs} \tag{9}$$

and

$$\dot{\epsilon}^T_{ij} = M_{ij} \dot{T} \tag{10}$$

with

$$M_{ij} = \frac{-\partial^2 \Phi}{\partial \sigma_{ij} \partial T} = \left[\frac{-\partial^2 \bar{E}(\sigma_{ij})}{\partial \sigma_{ij} \partial T} + \frac{\delta_{ij}}{3} \omega_{\tan} \right] \tag{11}$$

and

$$\omega_{\tan} = \omega + \frac{\partial \omega}{\partial T}(T - T_o) \tag{12}$$

denoting the instantaneous coefficient of thermal expansion, and $\dot{\epsilon}^I_{ij}$ (the inelastic strain rate) is defined separately using the concept of a complementary dissipation potential $\Omega(\sigma_{ij}, \alpha_\gamma, T)$. Whereby, given an

$$\Omega = \Omega(\sigma_{ij}, \alpha_\gamma, T) \tag{13}$$

and using the Clausius-Duhem inequality[5]; the flow law becomes

$$\dot{\epsilon}^I_{ij} = \frac{\partial \Omega}{\partial \sigma_{ij}} \tag{14}$$

and the evolutionary laws for the thermodynamic conjugate internal state variables are:

$$\dot{A}_\gamma = -\frac{\partial \Omega}{\partial \alpha_\gamma} \tag{15}$$

Utilizing eqn. (4) the internal constitutive rate equations for the internal state variables are obtained,

$$\dot{\alpha}_\gamma = L_{\gamma\xi}\left[\dot{A}_\xi - \theta_\xi \dot{T}\right] \tag{16}$$

where

$$L_{\gamma\xi} = [Q_{\gamma\xi}]^{-1} = \left[\frac{-\partial^2 \Phi}{\partial \alpha_\xi \partial \alpha_\gamma}\right]^{-1} \tag{17}$$

Thus, eqns. (14) and (15) represent the flow and evolutionary laws, for an assumed $\Omega = \Omega(\sigma_{ij}, \alpha_\gamma, T)$, and eqn. (16) the internal constitutive rate equations, given a Gibb's potential Φ, wherein both potentials are directly linked through the internal state variables α_γ. The specific forms selected thus far for both the Gibb's and complementary dissipation potentials resulted in a fully associative, multiaxial, nonisothermal, unified **GVIPS** (**G**eneralized **VI**scoplasticity with **P**otential **S**tructure) model with nonlinear kinematic hardening [6], [7].

During the detailed experimental program to specify the required material functions and characterize the associated material parameters for **TIMETAL 21S**[1], an advanced titanium-based matrix commonly used in titanium matrix composites (TMCs), it was discovered that **TIMETAL 21S** exhibited both a time and temperature dependent reversible (linear viscoelastic) and irreversible (viscoplastic) domain. These reversible and irreversible domains are posited to be delineated by temperature dependent threshold surfaces, as illustrated in Figure 1 for low, mid and high temperature regimes. In particular, as opposed to the purely time independent (elastic) behavior within the inner most threshold surface of Fig. 1b, two additional time dependent (reversible and irreversible mechanisms) will be activated upon traversing the two threshold surfaces shown. As our previous work has focused on the specification and characterization of the irreversible domain (i.e., eqns. (13)-(17)) the primary objective of the present study will be to construct, within the context of a complete potential structure, a multiaxial, nonisothermal viscoelastic model to describe the reversible strain component, see eqn. (9), of the total strain decomposition.

Clearly, this extension represents a very difficult problem [[8],[9]] in view of the multitude of choices available through the general functional forms Φ and Ω, and the complex interaction between the newly desired reversible viscous response component and the previous elasto-viscoplastic contributions. In particular, this involves the selection of the **type** of additional internal state variables and/or parameters accounting for the new mechanism, and their corresponding implied **partitioning** format of the stress and strain variables (further elaborated on in the following perspective section), within the context

[1]TIMETAL 21S is a registered trademark of TIMET, Titanium Metals Corporation, Toronto, OH.

of **multiaxial** stress states and in conformity with any thermodynamic **admissability requirements** (see Section 5 and references [[8],[9]] for many pertinent controversial issues).

The specific model construction has been motivated by experimental observations as discussed in detail in Part II [10] of this report. As an example see Fig. 2 which illustrates the rate dependence of the uniaxially obtained Young's Modulus as a function of temperature. Clearly at elevated temperature the Young's Modulus becomes increasingly rate dependent, thus indicating a need to include some type of viscoelastic influence into the deformation model at these temperatures. Another important observation, as shown in Fig. 2 of Part II [10], is the purely transient time dependent behavior of **TIMETAL 21S** with no steady state behavior being exhibited within the reversible strain domain of this material.

Other observations of a similar nature as above, i.e., marked rate and time-dependency in the so-called **quasilinear** range (at relatively low stress levels) have also been made by other investigators, motivating a number of extensions in constitutive theories. For example, these include distinctive static and dynamic moduli, reflecting the load-frequency-dependent behavior [11]-[12], and the use of an "initial" primary creep response component as extension of the well-known model of viscoplasticity theory based on overstress[13].

An outline of the remainder of the paper is as follows: In section 2 we discuss the significance of deciding **a priori** how one will partition the required stress and strain components and how this selection will influence our overall objective. In section 3 a specific multiaxial, nonisothermal, linear viscoelastic model of the internal-state-variable type is developed and then reduced and analyzed in section 4. In sections 5 and 6 numerous generalizations pertaining to both the theoretical foundation and numerical implementation are discussed. Lastly in section 7 a parametric study is conducted using the simplification (section 4) of the specific model developed in section 3 to illustrate the importance of a key assumption (i.e., equality of the Poisson's ratio's) and to identify important factors in the actual characterization of the specific-model put forth.

2 Perspective

Traditionally, for the small-deformation problems considered here, the total strain has been partitioned into an elastic (reversible), an inelastic (irreversible) and thermal (reversible) strain component, that is:

$$e_{ij} = \epsilon_{ij}^{R} + \epsilon_{ij}^{IR} + \epsilon_{ij}^{T} \tag{18}$$

where the inelastic strain corresponds to such physical phenomena as time-independent plastic strain or time-dependent viscoplastic strain (sometimes referred to as creep strain). Whether a material's phenomenological behavior is simple or complex, a mechanical model is often of great help in the visualization of that behavior. Here we want to discuss four such one-dimensional mechanical representations so as to put into perspective

previous work and motivate the construction of the present viscoelastic model. To this end, as shown in Fig. 3, a viscous element is shown pictorially by a dashpot whereas a linear-elastic element is pictured as a spring. For each element of the mechanical model, change in length represents strain in the material and force represents stress.

Let us begin with a uniaxial mechanical model that is representative of numerous internal state variable viscoplastic models available in the literature (e.g.,[4]), in particular the recent unified **GVIPS** model put forth by the authors[[6], [7]]. Fig. 3a presents a generalized nonlinear four element model (a spring in series with a nonlinear Maxwell element in parallel with a nonlinear dashpot) in which the strain is partitioned into an elastic and inelastic strain component; wherein implicit in the inelastic strain component is a partitioning of the stress into an internal stress (α) and effective stress ($\sigma - \alpha$) component. The resulting system of differential equations (total strain, flow, and evolution laws) are also shown in Fig. 3a, where it is clear that the flow and evolutionary laws are identical in structure (provided that the material parameters (e.g., E_1, η_2) are appropriately modified to become state dependent) to the **GVIPS** form, e.g., in the evolutionary law a competitive mechanism between hardening and thermal recovery is present.

Conversely, if we examine the classical four element (non)linear viscoelastic model [[14],[11]], as illustrated in Fig. 3b, which is capable of producing a similar elastic, primary and secondary creep history, we see that the resulting form of the flow and evolution laws are quite different. This difference is predicated upon the further partitioning of the inelastic strain component into a primary and secondary component, achieved by placing a Kelvin model in series with a dashpot, thus resulting in a more complex flow law and restrictive evolution law. Comparing the resulting equations of Fig. 3b with that of Fig. 3a, it is immediately apparent that one should **not** assume (as is often done) that commonly employed unified viscoplastic formulations (of which Fig. 3a is representative) are merely extensions of this classical four element configuration to the irreversible domain.

As the emphasis in this study will be on developing a transient viscoelastic model, let us compare two three element configurations that give the same "classical"[2] uniaxial behavior in both creep and relaxation. The first can be immediately obtained from a truncation of the four element model presented in Fig. 3b. This truncation is obtained by setting η_4 to infinity and results, as before, in a partitioning of the applied strain into an elastic and primary creep regime. Alternatively, one can construct a complementary configuration in which the stress (instead of the strain) is partitioned into an elastic and viscous part. This model is known as the standard linear (n = 1) solid model[11] and is shown in Fig. 4a along with the pertinent one-dimensional governing equations. The one dimensional solution to the governing systems of equations for Figs. 3b and 4a, for the special case of linear (n = 1) viscoelasticity, is illustrated in Fig. 4b for both models and will be subsequently used to validate the one dimensional simplification of

[2]By classical we mean, in conformity with the classical rheological model we interpret the uniaxial results to imply complete neglection of the strain component interactions (i.e., no Poisson's effect and a truly one-dimensional response)

the proposed multiaxial theory. Clearly, both approaches (i.e., partitioning of the stress or strain) are capable of producing the desired uniaxial response (see the table in Fig. 4b); however, with an eye toward integrating the resulting viscoelastic theory with the author's previously proposed **GVIPS** model, the partitioning of the stress (standard linear model) approach is preferred.

This preference is obvious when one recalls the four element model of Fig. 3a, the decomposition of the total strain into reversible and irreversible components, and our desire to **maintain** the current **GVIPS** representation for the irreversible component of strain. Consequently, we will merely replace the single spring element in Fig. 3a with the standard linear model of Fig. 4a, as illustrated in Fig. 5. Mathematically this is accomplished by employing an additive decomposition for the two underlying thermodynamic potentials (i.e., complementary energy/ Gibb's (see eqn. 1) and dissipation functions (see eqn.. 13) into reversible and irreversible parts, that is $\Phi = \Phi_R + \Phi_{IR}$ and $\Omega = \Omega_R + \Omega_{IR}$; where $\Phi_{IR} = -\sigma_{ij}\epsilon^I_{ij} - \bar{H}\ (\alpha_\gamma, T)$ and $\Omega_{IR} = \Omega(\sigma_{ij}, \alpha_\gamma, T)$ are defined as before in eqns. (2) and (13). Henceforth, we will concentrate only on the construction of the multiaxial, nonisothermal, linear viscoelastic representation of the now (time-dependent) viscous reversible strain component, i.e., Φ_R and Ω_R .

3 Multiaxial Nonisothermal Theory

Here we will restrict our discussion to the reversible viscous part, where the corresponding functions Φ_R and Ω_R are assumed **a priori** to be in conformity with Fig. 4a. Furthermore, for conciseness the discussion is limited to a case involving small deformations (in which the initial state is assumed to be stress free) and a **linear** viscous element (which is in accordance with the experimental evidence described in Part II). A Cartesian coordinate reference frame and index notation are utilized (repeated Roman subscripts imply summation).

The reversible contribution to the Gibb's potential takes the following partitioned form

$$\Phi_R = \Phi_R(\sigma^m_{ij}, \sigma^s_{ij}, T) = -\frac{1}{2}\sigma^s_{ij}E^{-1}_{ijrs}\sigma^s_{rs} - \frac{1}{2}\sigma^m_{ij}M^{-1}_{ijrs}\sigma^m_{rs} - \sigma^m_{ij}\varepsilon^d_{ij} - \frac{\sigma^s_{kk} + \sigma^m_{kk}}{3}\omega(T - T_o) \quad (19)$$

where the first term represents the stored energy in the spring element, the second, the stored energy in the Maxwell element, and the third, the energy dissipated by the dashpot within the Maxwell element. The **equations of state** for the conjugate strains (i.e., strains in the spring and Maxwell elements) can be obtained by differentiating with respect to the associated variables, σ^s_{ij} and σ^m_{ij}, respectively; i.e., $e^s_{ij} = \frac{-\partial\Phi_R}{\partial\sigma^s_{ij}}$ and $e^m_{ij} = \frac{-\partial\Phi_R}{\partial\sigma^m_{ij}}$. In rate form,

$$\dot{e}^s_{ij} = \frac{d}{dt}\left(\frac{-\partial\Phi_R}{\partial\sigma^s_{ij}}\right) = E^{-1}_{ijrs}\dot{\sigma}^s_{rs} + \theta^E_{ij}\dot{T} \quad (20)$$

$$\dot{e}^m_{ij} = \frac{d}{dt}\left(\frac{-\partial \Phi_R}{\partial \sigma^m_{ij}}\right) = M^{-1}_{ijrs}\dot{\sigma}^m_{rs} + \dot{\varepsilon}^d_{ij} + \theta^M_{ij}\dot{T} \tag{21}$$

with

$$\theta^E_{ij} = \left[\frac{-\partial E^{-1}_{ijrs}}{\partial T}\sigma^s_{rs} + \frac{\delta_{ij}}{3}\omega_{\tan}\right] \tag{22}$$

$$\theta^M_{ij} = \left[\frac{-\partial M^{-1}_{ijrs}}{\partial T}\sigma^m_{rs} + \frac{\delta_{ij}}{3}\omega_{\tan}\right] \tag{23}$$

where $\omega_{\tan}$ denotes the instantaneous coefficient of thermal expansion (see eqn. (12)), and $\dot{\varepsilon}^d_{ij}$ (the dashpot strain rate) is defined separately using the concept of a complementary viscoelastic dissipation potential $\Omega_R(\sigma^m_{ij}, T)$.

Given

$$\Omega_R = \frac{1}{2}\sigma^m_{ij}\eta^{-1}_{ijrs}\sigma^m_{rs} \tag{24}$$

the **flow law** for the dashpot becomes

$$\dot{\varepsilon}^d_{ij} = \frac{-\partial \Omega_R}{\partial \sigma^m_{ij}} = \eta^{-1}_{ijrs}\sigma^m_{rs} \tag{25}$$

Thus substituting eqn. (25) into eqn. (21) and making use of the fact that

$$\sigma^m_{ij} = \sigma_{ij} - \sigma^s_{ij} \tag{26}$$

due to the partitioning of the stress, eqn. (21) becomes,

$$\dot{e}^m_{ij} = M^{-1}_{ijrs}(\dot{\sigma}_{rs} - \dot{\sigma}^s_{rs}) + \eta^{-1}_{ijrs}(\sigma_{rs} - \sigma^s_{rs}) + \theta^M_{ij}\dot{T} \tag{27}$$

As a kinematic compatibility constraint, the total strain is equivalent to the strain in the spring and in the Maxwell element, i.e.,

$$e_{ij} = e^m_{ij} = e^s_{ij} \tag{28}$$

the evolution of the internal stress(σ^s_{ij}) can be derived.

$$\dot{\sigma}^s_{kl} = \overline{EM}_{klij}\{M^{-1}_{ijrs}\dot{\sigma}_{rs} + \eta^{-1}_{ijrs}(\sigma_{rs} - \sigma^s_{rs}) + \hat{\theta}_{ij}\dot{T}\} \tag{29}$$

where

$$\overline{EM}_{klij} = \{E^{-1}_{klij} + M^{-1}_{klij}\}^{-1} \tag{30}$$

and

$$\hat{\theta}_{ij} = \frac{-\partial E^{-1}_{ijrs}}{\partial T}\sigma^s_{rs} + \frac{\partial M^{-1}_{ijrs}}{\partial T}(\sigma_{rs} - \sigma^s_{rs}) \tag{31}$$

Finally, using eqns. (20) and (29) we obtain the desired multiaxial nonisothermal viscoelastic stress-strain expression,

$$\dot{e}_{ij} = E^{-1}_{ijkl}[\overline{EM}_{klmn}\{M^{-1}_{mnrs}\dot{\sigma}_{rs} + \eta^{-1}_{mnrs}(\sigma_{rs} - \sigma^s_{rs}) + \hat{\theta}_{mn}\dot{T}\}] + \theta^E_{ij}\dot{T} \tag{32}$$

with the evolution of internal stress given by eqn. (29).

Now assuming an **isotropic** material, the general form for the isotropic material tensor (in terms of the bulk modulus K and shear modulus G) is as follows:

$$C_{ijkl} = (K_C - \frac{2}{3}G_C)\delta_{ij}\delta_{kl} + 2G_C(\delta_{ik}\delta_{jl} + \delta_{il}\delta_{jk}) \tag{33}$$

where the subscript on the bulk and shear modulus (i.e., C) will always be indicative of the particular material tensor being replaced (e.g., C_{ijkl}). Similarly, one can write the general isotropic stress-strain relations as follows:

$$\sigma_{ij} = Ke_{kk}\delta_{ij} + 2G(e_{ij} - \frac{1}{3}e_{kk}\delta_{ij}) \tag{34}$$

or

$$e_{ij} = \frac{1}{9K}\sigma_{kk}\delta_{ij} + \frac{1}{2G}(\sigma_{ij} - \frac{1}{3}\sigma_{kk}\delta_{ij}) \tag{35}$$

Utilizing these above relations and performing a number of algebraic manipulations on eqn. (32) the desired isotropic, multiaxial, nonisothermal, viscoelastic stress-strain expressions can be obtained, that is

$$\begin{aligned} K_E\dot{e}_{kk}\delta_{ij} + 2G_E(\dot{e}_{ij} - \frac{1}{3}\dot{e}_{kk}\delta_{ij}) \;=\; & \frac{1}{3}\left[\frac{K_{EM}}{K_M} - \frac{G_{EM}}{G_M}\right]\dot{\sigma}_{kk}\delta_{ij} + \frac{G_{EM}}{G_M}\dot{\sigma}_{ij} + \\ & \frac{1}{3}\left[\frac{K_{EM}}{K_\eta} - \frac{G_{EM}}{G_\eta}\right](\sigma_{rr} - \sigma^s_{rr})\delta_{ij} + \frac{G_{EM}}{G_\eta}(\sigma_{ij} - \sigma^s_{ij}) + \\ & \left(\begin{array}{l} \frac{1}{3}\left[\frac{K_{EM}}{K^T_M} - \frac{G_{EM}}{G^T_M}\right](\sigma_{rr} - \sigma^s_{rr})\delta_{ij} - \frac{1}{3}\left[\frac{K_{EM}}{K^T_E} - \frac{G_{EM}}{G^T_E}\right]\sigma^s_{rr}\delta_{ij} + \\ \frac{G_{EM}}{G^T_M}(\sigma_{ij} - \sigma^s_{ij}) - \frac{G_{EM}}{G^T_E}\sigma^s_{ij} + \frac{1}{3}\left[\frac{K_E}{K^T_E} - \frac{G_E}{G^T_E}\right]\sigma^s_{rr}\delta_{ij} + \frac{G_E}{G^T_E}\sigma^s_{ij} \end{array}\right)\dot{T} \end{aligned} \tag{36}$$

where the notation for the derivative with respect to temperature of the bulk and shear modulus is defined as

$$K^T_{E,\,M} = -\frac{K^2_{E,\,M}(T)}{\frac{\partial K_{E,\,M}(T)}{\partial T}} \tag{37}$$

$$G^T_{E,\,M} = -\frac{G^2_{E,\,M}(T)}{\frac{\partial G_{E,\,M}(T)}{\partial T}} \tag{38}$$

such that if K and G are temperature independent, i.e., $\frac{\partial}{\partial T} = 0$, K^T_E, K^T_M and G^T_E, G^T_M are infinity and thus the temperature rate term ($\dot{T}$) will vanish.

4 Subspace Simplification

If we consider a triaxial (principle) state of stress and isothermal conditions ($\dot{T}$=0), eqns. (36) can be transformed into the following system

$$\begin{aligned} \mathbf{Y} &= \mathbf{DX} \\ \dot{\mathbf{X}} + \mathbf{AX} &= \mathbf{AL} + \bar{\mathbf{A}}\dot{\mathbf{L}} \end{aligned} \tag{39}$$

with $(\dot{\cdot})$ denoting the time derivative and

$$\mathbf{Y} = \begin{pmatrix} e_{11} \\ e_{22} \\ e_{33} \end{pmatrix}, \qquad \mathbf{X} = \begin{pmatrix} \sigma^s_{11} \\ \sigma^s_{22} \\ \sigma^s_{33} \end{pmatrix}, \qquad \mathbf{L} = \begin{pmatrix} \sigma_{11} \\ \sigma_{22} \\ \sigma_{33} \end{pmatrix} \tag{40}$$

$$\mathbf{D} = \frac{3K_E + G_E}{9G_E K_E} \begin{bmatrix} 1 & -\frac{(3K_E - 2G_E)}{2(3K_E + G_E)} & -\frac{(3K_E - 2G_E)}{2(3K_E + G_E)} \\ -\frac{(3K_E - 2G_E)}{2(3K_E + G_E)} & 1 & -\frac{(3K_E - 2G_E)}{2(3K_E + G_E)} \\ -\frac{(3K_E - 2G_E)}{2(3K_E + G_E)} & -\frac{(3K_E - 2G_E)}{2(3K_E + G_E)} & 1 \end{bmatrix} \tag{41}$$

$$\mathbf{A} = \begin{bmatrix} b & a & a \\ a & b & a \\ a & a & b \end{bmatrix}, \qquad \bar{\mathbf{A}} = \begin{bmatrix} \bar{b} & \bar{a} & \bar{a} \\ \bar{a} & \bar{b} & \bar{a} \\ \bar{a} & \bar{a} & \bar{b} \end{bmatrix} \tag{42}$$

where

$$a = \frac{1}{3}\left[\frac{K_{EM}}{K_\eta} - \frac{G_{EM}}{G_\eta}\right], \qquad b = \frac{1}{3}\left[\frac{K_{EM}}{K_\eta} + 2\frac{G_{EM}}{G_\eta}\right] \tag{43}$$

$$\bar{a} = \frac{1}{3}\left[\frac{K_{EM}}{K_M} - \frac{G_{EM}}{G_M}\right], \qquad \bar{b} = \frac{1}{3}\left[\frac{K_{EM}}{K_M} + 2\frac{G_{EM}}{G_M}\right] \tag{44}$$

Now as the matrix $\mathbf{A}$ is real, symmetric and positive definite, then we know that 1) its eigenvalues $(\lambda_1, \lambda_2, ...)$ are all real and positive, 2) its eigenvectors can be chosen orthonormal and 3) $\mathbf{A} = \mathbf{N}\Lambda\mathbf{N}^{-1}$where Λ is a diagonal matrix containing the eigenvalues of $\mathbf{A}$. Consequently, if we let

$$\mathbf{Z} = \mathbf{N}^{-1}\mathbf{X}, \qquad \dot{\mathbf{Z}} = \mathbf{N}^{-1}\dot{\mathbf{X}} \tag{45}$$

eqn. (39) can be rewritten as

$$\dot{\mathbf{Z}} + \Lambda\mathbf{Z} = \mathbf{N}^{-1}(\mathbf{AL} + \bar{\mathbf{A}}\dot{\mathbf{L}}) \tag{46}$$

and solving for Z we obtain

$$\mathbf{Z} = \mathbf{C}e^{-\Lambda t} + \mathbf{Z}^{particular} \tag{47}$$

where the form of $\mathbf{Z}^{particular}$ will depend upon the applied loading vector $\mathbf{L}$. Finally, transforming back to the real space X, we obtain the desired general solution

$$\mathbf{X} = \mathbf{N}\mathbf{C}e^{-\mathbf{\Lambda}t} + \mathbf{X}^{particular} \tag{48}$$

with

$$\mathbf{Y} = \mathbf{D}\mathbf{N}\mathbf{C}e^{-\mathbf{\Lambda}t} + \mathbf{D}\mathbf{X}^{particular}$$

4.1 Creep History

As an example, let us examine the case when the applied load is linear in time, i.e.,

$$\begin{aligned} \mathbf{L} &= \boldsymbol{\beta}t + \mathbf{L}^* \\ \dot{\mathbf{L}} &= \boldsymbol{\beta} \end{aligned}$$

wherein the (3x1) vectors $\boldsymbol{\beta}$ and $\mathbf{L}^*$ are prescribed time invariant constants; thus eqn. (46) maybe rewritten as

$$\dot{\mathbf{Z}} + \mathbf{\Lambda}\mathbf{Z} = \mathbf{N}^{-1}[\mathbf{A}\boldsymbol{\beta}t + \bar{\mathbf{A}}\boldsymbol{\beta} + \mathbf{A}\mathbf{L}^*]. \tag{49}$$

Solving for the particular solution of eqn. (49) we obtain

$$\mathbf{Z}^p = \mathbf{\Lambda}^{-1}\left[\left(t\mathbf{I} - \mathbf{\Lambda}^{-1}\right)\mathbf{N}^{-1}\mathbf{A}\boldsymbol{\beta} + \mathbf{N}^{-1}(\bar{\mathbf{A}}\boldsymbol{\beta} + \mathbf{A}\mathbf{L}^*)\right] \tag{50}$$

and transforming back to $\mathbf{X}$ we obtain

$$\mathbf{X}^p = \boldsymbol{\beta}t - \mathbf{A}^{-1}[\boldsymbol{\beta} - \bar{\mathbf{A}}\boldsymbol{\beta}] + \mathbf{L}^* \tag{51}$$

so that in this case

$$\mathbf{X} = \mathbf{N}e^{-\mathbf{\Lambda}t}\mathbf{C} + \boldsymbol{\beta}t - \mathbf{A}^{-1}[\boldsymbol{\beta} - \bar{\mathbf{A}}\boldsymbol{\beta}] + \mathbf{L}^* \tag{52}$$

where the coefficient vector $\mathbf{C}$ must still be solved for, given a set of initial conditions.

For instance assuming that we start at zero stress and apply a constant load rate and then at time equal t_0 hold the load constant (i.e., a typical stress controlled creep test) we would obtain the following, that is for: $\mathbf{L}^* = \mathbf{0}$ and $\mathbf{X} = \mathbf{0}$, $\boldsymbol{\beta} \neq \mathbf{0}$ at $t = 0$ we get

$$\mathbf{C} = \mathbf{N}^{-1}\mathbf{A}^{-1}\left[\boldsymbol{\beta} - \bar{\mathbf{A}}\boldsymbol{\beta}\right] \tag{53}$$

and

$$\mathbf{X} = \left(\mathbf{N}e^{-\mathbf{\Lambda}t}\mathbf{N}^{-1} - \mathbf{I}\right)\mathbf{A}^{-1}\left[\boldsymbol{\beta} - \bar{\mathbf{A}}\boldsymbol{\beta}\right] + \boldsymbol{\beta}t; \quad 0 \leq t \leq t_0 \tag{54}$$

and for $t \geq t_0$, ($\boldsymbol{\beta} = \mathbf{0}$ and $\mathbf{L}^* \neq \mathbf{0}$) we get

$$\mathbf{C} = \left[\mathbf{N}e^{-\mathbf{\Lambda}t_0}\right]^{-1}\left[\mathbf{X}_{t_0} - \mathbf{L}^*\right] \tag{55}$$

and

$$\mathbf{X} = \mathbf{N}e^{-\mathbf{\Lambda}t}\left\{\left[\mathbf{N}e^{-\mathbf{\Lambda}t_0}\right]^{-1}\left[\mathbf{X}_{t_0} - \mathbf{L}^*\right]\right\} + \mathbf{L}^*; \quad t \succeq t_0 \tag{56}$$

where

$$\mathbf{X}_{t_0} = \left(\mathbf{N}e^{-\mathbf{\Lambda} t_0}\mathbf{N}^{-1} - \mathbf{I}\right)\mathbf{A}^{-1}\left[\boldsymbol{\beta} - \bar{\mathbf{A}}\boldsymbol{\beta}\right] + \boldsymbol{\beta} t_0 \tag{57}$$

with

$$\mathbf{Y} = \mathbf{D}\mathbf{X}$$

as before. Or alternatively, we could assume the classic creep case involving an instantaneous load-up to a constant stress value $\mathbf{L}^* \neq \mathbf{0}$ at $t_0 = 0$ and therefore after taking the appropriate limits as t_0 approaches zero (i.e., $\lim \mathbf{X}_{t_0} = \bar{\mathbf{A}}\boldsymbol{\beta}^*$) eqn. (55) becomes

$$\mathbf{C} = \mathbf{N}^{-1}[\bar{\mathbf{A}}\boldsymbol{\beta}^* - \mathbf{L}^*] \tag{58}$$

and eqn. (56)

$$\mathbf{X} = \mathbf{N}e^{-\mathbf{\Lambda} t}\mathbf{N}^{-1}[\bar{\mathbf{A}}\boldsymbol{\beta}^* - \mathbf{L}^*] + \mathbf{L}^* \tag{59}$$

and if $\boldsymbol{\beta}^* = \mathbf{L}^*$:

$$\mathbf{X} = \{\mathbf{N}e^{-\mathbf{\Lambda} t}\mathbf{N}^{-1}[\bar{\mathbf{A}} - \mathbf{I}] + \mathbf{I}\}\mathbf{L}^* \tag{60}$$

4.1.1 Uniaxial Simplification

Now if we further restrict ourselves to a purely uniaxial creep loading (e.g., $L_1^* = \sigma_{11} = \sigma^*$ & $\dot{\sigma}_{11} = \beta_1 = \frac{\sigma^*}{t_0}$; $\sigma_{22} = \sigma_{33} = \dot{\sigma}_{22} = \dot{\sigma}_{33} = 0$) case and make use of the symmetry resulting from the previous assumption of an isotropic material (i.e., $\sigma_{22}^s = \sigma_{33}^s$, $\dot{\sigma}_{22}^s = \dot{\sigma}_{33}^s$), the various matrices and vectors take on the following reduced forms:

$$\mathbf{A} = \begin{bmatrix} b & 2a \\ a & a+b \end{bmatrix} = \frac{1}{3}\begin{bmatrix} K^* + 2G^* & 2K^* - 2G^* \\ K^* - G^* & 2K^* + G^* \end{bmatrix} \tag{61}$$

$$\mathbf{A}^{-1} = \frac{1}{3G^*K^*}\begin{bmatrix} G^* + 2K^* & -2(K^* - G^*) \\ -(K^* - G^*) & 2G^* + K^* \end{bmatrix} \tag{62}$$

$$\mathbf{\Lambda} = \begin{bmatrix} K^* & 0 \\ 0 & G^* \end{bmatrix}, \qquad \mathbf{N} = \begin{bmatrix} \frac{1}{\sqrt{2}} & \frac{2}{\sqrt{5}} \\ \frac{1}{\sqrt{2}} & \frac{-1}{\sqrt{5}} \end{bmatrix}, \qquad \mathbf{N}^{-1} = \frac{-\sqrt{10}}{3}\begin{bmatrix} \frac{-1}{\sqrt{5}} & -\frac{2}{\sqrt{5}} \\ -\frac{1}{\sqrt{2}} & \frac{1}{\sqrt{2}} \end{bmatrix} \tag{63}$$

$$\bar{\mathbf{A}} = \begin{bmatrix} \bar{b} & 2\bar{a} \\ \bar{a} & \bar{a}+\bar{b} \end{bmatrix} = \frac{1}{3}\begin{bmatrix} \bar{K}^* + 2\bar{G}^* & 2\bar{K}^* - 2\bar{G}^* \\ \bar{K}^* - \bar{G}^* & 2\bar{K}^* + \bar{G}^* \end{bmatrix} \tag{64}$$

$$\boldsymbol{\beta} = \frac{\sigma^*}{t_0}\begin{Bmatrix} 1 \\ 0 \end{Bmatrix}, \qquad \boldsymbol{\beta}^* = \mathbf{L}^* = \sigma^*\begin{Bmatrix} 1 \\ 0 \end{Bmatrix} \tag{65}$$

where

$$K^* = \frac{K_{EM}}{K_\eta}, \quad G^* = \frac{G_{EM}}{G_\eta}, \quad \bar{K}^* = \frac{K_{EM}}{K_M}, \quad \bar{G}^* = \frac{G_{EM}}{G_M} \tag{66}$$

So that

$$\mathbf{N}e^{-\mathbf{\Lambda}t}\mathbf{N}^{-1} = \frac{1}{3}\begin{bmatrix} e^{-K^*t} + 2e^{-G^*t} & 2\left(e^{-K^*t} - e^{-G^*t}\right) \\ e^{-K^*t} - e^{-G^*t} & 2e^{-K^*t} + e^{-G^*t} \end{bmatrix} \tag{67}$$

$$\mathbf{A}^{-1}\left[\boldsymbol{\beta} - \bar{\mathbf{A}}\boldsymbol{\beta}\right] = \frac{\sigma^*}{9G^*K^*t_0}\begin{bmatrix} \left[1 - \left(\bar{K}^* + 2\bar{G}^*\right)\right](2K^* + G^*) + 2(K^* - G^*)(\bar{K}^* - \bar{G}^*) \\ -\left[1 - \left(\bar{K}^* + 2\bar{G}^*\right)\right](K^* - G^*) - (K^* + 2G^*)(\bar{K}^* - \bar{G}^*) \end{bmatrix} \tag{68}$$

and in the classic creep case (i.e., eqn. (60))

$$\mathbf{X} = \frac{\sigma^*}{3}\begin{bmatrix} 3 + (\bar{K}^* - 1)e^{-K^*t} - 2(1 - \bar{G}^*)e^{-G^*t}) \\ (\bar{K}^* - 1)e^{-K^*t} + (1 - \bar{G}^*)e^{-G^*t} \\ (\bar{K}^* - 1)e^{-K^*t} + (1 - \bar{G})e^{-G^*t} \end{bmatrix} \tag{69}$$

and

$$Y = \frac{\sigma^*}{E_S}\begin{bmatrix} 1 + \frac{1}{3}(1 - 2\nu_s)(\bar{K}^* - 1)e^{-K^*t} - \frac{2}{3}(1 + \nu_s)(1 - \bar{G}^*)e^{-G^*t}) \\ -\nu_s + \frac{1}{3}(1 - 2\nu_s)(\bar{K}^* - 1)e^{-K^*t} + \frac{1}{3}(1 + \nu_s)(1 - \bar{G}^*)e^{-G^*t} \\ -\nu_s + \frac{1}{3}(1 - 2\nu_s)(\bar{K}^* - 1)e^{-K^*t} + \frac{1}{3}(1 + \nu_s)(1 - \bar{G}^*)e^{-G^*t} \end{bmatrix} \tag{70}$$

where

$$K^* = E^*\nu, \quad G^* = E^*\nu^*, \quad \bar{K}^* = \bar{E}^*\bar{\nu}, \quad \bar{G}^* = \bar{E}^*\bar{\nu}^* \tag{71}$$

$$E^* = \frac{\overline{EM}}{\eta} = \left(\frac{E_M E_S}{E_M + E_S}\right)\frac{1}{\eta}, \quad \bar{E}^* = \frac{\overline{EM}}{E_M} = \frac{E_S}{E_M + E_S} \tag{72}$$

$$\nu = \frac{(1 - 2\nu_\eta)}{(1 - 2\nu_{EM})}, \quad \nu^* = \frac{(1 + \nu_\eta)}{(1 + \nu_{EM})}, \quad \nu_{EM} = \frac{E_M\nu_s + E_S\nu_M}{E_S + E_M} \tag{73}$$

$$\bar{\nu} = \frac{(1 - 2\nu_M)}{(1 - 2\nu_{EM})}, \quad \bar{\nu}^* = \frac{(1 + \nu_M)}{(1 + \nu_{EM})} \tag{74}$$

and $\mathbf{D}$ was taken to be

$$\mathbf{D} = \frac{1}{E_s}\begin{bmatrix} 1 & -\nu_s & -\nu_s \\ -\nu_s & 1 & -\nu_s \\ -\nu_s & -\nu_s & 1 \end{bmatrix} \tag{75}$$

Now in order to recover the "classical" one-dimensional linear viscoelastic solution for an instantaneously (step-function) applied creep load, see Fig.4b, all Poisson's ratios must be taken to be zero (i.e., $\nu_s = \nu_m = \nu_\eta = 0$, leading to a=0 and $K^* = G^* = E^*$, $\bar{K}^* = \bar{G}^* = \bar{E}^*$). Consequently, eqn. (70) reduces directly to the simple expression given in Fig. 4b, that is

$$Y = \frac{\sigma^*}{E_S}\begin{bmatrix} 1 - (\bar{E}^* - 1)e^{-E^*t} \\ 0 \\ 0 \end{bmatrix} \tag{76}$$

where E^* (i.e., $\frac{1}{\tau}$) and $\bar{E}^*$ are defined in eqn.(72). Alternatively, we can rewrite eqn. (70) in terms of individual Poisson's ratios and element stiffnesses, to obtain the initial or instantaneous response (that is at t=0):

$$Y = C_0 \begin{bmatrix} (1+\alpha) - (1+2\nu_m)(\nu_m + \alpha\nu_s) - 2\nu_s[(\nu_m + \alpha\nu_s) - \nu_m(1+\alpha)] \\ (\nu_m + \alpha\nu_s)(1+2\nu_m\nu_s) + (1+\alpha)[\nu_s(\nu_m - 1) - \nu_m] \\ (\nu_m + \alpha\nu_s)(1+2\nu_m\nu_s) + (1+\alpha)[\nu_s(\nu_m - 1) - \nu_m] \end{bmatrix} \tag{77}$$

where

$$C_0 = \frac{\sigma^*}{E_S[(1+\alpha) - 2(\nu_m + \alpha\nu_s)][(1+\alpha) + (\nu_m + \alpha\nu_s)]}$$

Then if we assume $\nu_s \neq \nu_m$, but $\alpha = 1$ then,

$$Y = \frac{\sigma^*}{2E_S[(2 - (\nu_m + \nu_s) - (\nu_m + \nu_s)^2]} \begin{bmatrix} 2 - (\nu_m + \nu_s) - (2\nu_s^2 + 2\nu_m^2) \\ -\nu_s(1+\nu_m)(1-2\nu_m) + -\nu_m(1+\nu_s)(1-2\nu_s) \\ -\nu_s(1+\nu_m)(1-2\nu_m) + -\nu_m(1+\nu_s)(1-2\nu_s) \end{bmatrix} \tag{78}$$

or if we take $\nu_s = \nu_m = \nu$, but $\alpha \neq 1$ then,

$$Y = \frac{\sigma^*}{E_s(1+\alpha)} \begin{Bmatrix} 1 \\ -\nu \\ -\nu \end{Bmatrix} = \frac{\sigma^*}{E_s + E_m} \begin{Bmatrix} 1 \\ -\nu \\ -\nu \end{Bmatrix} \tag{79}$$

Consequently, the above expressions provide us with an alternative means (instead of direct experimental measurement) to determine the proper assumption for the Poisson's ratios, given the experimentally measurable dynamic modulus. It is interesting to note that if the assumption of constant and equal Poisson's ratios is accurate then eqn. (79) proves that the dynamic modulus is equal to the summation of E_s and E_m, i.e., $E_0 = E_s + E_m$.

4.2 Relaxation History

Alternatively, considering a triaxial (principle) state of strain and isothermal conditions, a similar set of expressions as those shown in eqns. (39)-(60) can be obtained. That is,

$$\begin{aligned} \mathbf{X} &= \mathbf{D}^{-1}\mathbf{Y} \\ \dot{\mathbf{L}} + \mathbf{BL} &= \bar{\mathbf{B}}\dot{\mathbf{Y}} + \mathbf{BD}^{-1}\mathbf{Y} \end{aligned} \tag{80}$$

where

$$\begin{aligned} \mathbf{B} &= \bar{\mathbf{A}}^{-1}\mathbf{A} \\ \bar{\mathbf{B}} &= \bar{\mathbf{A}}^{-1}\mathbf{D}^{-1} \end{aligned}$$

and $\Lambda_B = \mathbf{N}_B^{-1}\mathbf{B}\mathbf{N}_B$ with N_B being the eigenvector matrix of $\mathbf{B}$. Then assuming the applied strain field is linear in time, i.e.,

$$\begin{aligned} \mathbf{Y} &= \boldsymbol{\zeta} t + \mathbf{Y}^* \\ \dot{\mathbf{Y}} &= \boldsymbol{\zeta} \end{aligned}$$

we obtain the counterparts to eqns. (54), (56), and (60), respectively:

$$\mathbf{L} = \left(\mathbf{N}_B e^{-\Lambda_B t}\mathbf{N}_B^{-1} - \mathbf{I}\right)\mathbf{B}^{-1}\left[\mathbf{D}^{-1}\boldsymbol{\zeta} - \bar{\mathbf{B}}\boldsymbol{\zeta}\right] + \mathbf{D}^{-1}\boldsymbol{\zeta} t; \quad 0 \le t \le t_0 \tag{81}$$

$$\mathbf{L} = \mathbf{N}_B e^{-\Lambda_B t}\left\{\left[\mathbf{N}_B e^{-\Lambda_B t_0}\right]^{-1}\left[\mathbf{L}_{t_0} - \mathbf{D}^{-1}\mathbf{Y}^*\right]\right\} + \mathbf{D}^{-1}\mathbf{Y}^*; \quad t \succeq t_0 \tag{82}$$

and

$$\mathbf{L} = \{\mathbf{N}_B e^{-\Lambda_B t}\mathbf{N}_B^{-1}[\bar{\mathbf{B}} - \mathbf{D}^{-1}] + \mathbf{D}^{-1}\}\mathbf{Y}^*; \qquad \text{if } t_0 = 0 \tag{83}$$

The above general triaxial forms will prove very useful in conducting parametric studies under multiaxial states of stress and in providing insight into identifying the most discriminating experimental validation test conditions. In fact, all the results to be given later are generated using these principle field expressions.

5 General Characteristics and Equivalent Hereditary Integral Representation

Largely motivated by the experimental observations alluded to earlier (see Fig. 2 and Part II) we have elected to focus our attention on a single internal dissipative mode in the above derivations. However, the underlying thermodynamic formalism [[5],[9]] is sufficiently general to provide for a number of possible extensions. Several such generalizations are described below, together with the exploitation of their "equivalent" integral forms within the modern theories of materials with memory; i.e., hereditary integral representations, e.g. [9]. In particular , a difficult question concerns here the proper conditions to be imposed on the kernels associated with general hereditary integrals, and in this connection the distinct advantages offered by the present formulation will become apparent.

5.1 Limiting and Equilibrium States

As a simple rheological interpretation the assumed structure of the (complementary) free energy, eqn.(19), leads to a local **additive** decomposition of the stress tensor into an **equilibrium** stress, σ^s, and a **non-equilibrium** stress, σ^m, see chapter 2 of [15] and Kremple formulation in [13]. The non-equilibrium stress is governed by a linear, dissipative, evolution equation exhibiting the well known **fading memory** phenomenon.. This is characterized by a viscous-like environment in which microstructural changes take place within a temperature dependent quasi-linear regime, as illustrated in Fig. 1.

In particular, for arbitrary deformations, from eqns. (26) and (29), the condition for thermodynamic equilibrium is when

$$\sigma^m \mid_{t\to\infty} = 0 \tag{84}$$

This in turn results in $\dot{\varepsilon}^d_{ij} \mid_{t\to\infty} = 0$ and hence the vanishing of the dissipation at equilibrium, i.e., $\Omega_R \mid_{t\to\infty} = 0$. This is in conformity with the **thermoelastic** (time independent reversible) **limit** put forth by Truesdell and Noll [5] wherein the thermodynamic process becomes reversible, and the material reacts fully thermoelastically. This limit is depicted schematically in Fig. 6 by the solid line, and the following one-dimensional expression , that is ,

$$e_{equil} = E_0^{-1}\sigma_{TI}(T) + E_\infty^{-1}\left\langle \sigma - \sigma_{TI}(T) \right\rangle \tag{85}$$

where E_0 is the initial (instantaneous or dynamic) stiffness modulus, E_∞ is the stiffness modulus at infinite time (E_s), σ_{TI} is the upper stress limit delineating time independent reversible behavior from time dependent, and $\langle\rangle$ denote Macauley bracket.

5.2 Model Generalizations

For simplicity, and without loss of generality, only the **isothermal** conditions are considered in the following discussions. Furthermore, for the case of isotropy (see also Remark 2) we assume all the fourth-order tensors of moduli **E**, **M**, $\boldsymbol{\eta}$ to be coaxial. This, together with the linear structure of eqns. (27) and (29), enables us to express the internal variable, σ^m, in terms of a simple convolution integral:

$$\boldsymbol{\sigma}^m = \int_0^t e^{\frac{-(t-s)}{\tau}} \frac{d}{ds}[\boldsymbol{\eta}^* \mathbf{E}^{-1}\boldsymbol{\sigma}]ds \tag{86}$$

or

$$\boldsymbol{\sigma}^m = \int_0^t e^{-\frac{(t-s)}{\rho}} \frac{d}{ds}[\boldsymbol{\eta}^* \mathbf{e}]ds \tag{87}$$

where $\overline{EM} = \frac{1}{\tau}\boldsymbol{\eta} = \boldsymbol{\eta}^*$, $M = \frac{1}{\rho}\boldsymbol{\eta} = \boldsymbol{\eta}^*$are assumed with τ and ρ as the positive relaxation times.

With this **convolution** representation many generalizations are possible once an appropriate choice of its kernel is made. For example, several relaxation times may be introduced by replacing the single exponential term in eqn. (86) with the **discrete-relaxation-spectrum** kernel,

$$K(t) = \sum_{j=1}^{N} e^{\frac{-t}{\tau_j}} \tag{88}$$

The most general form, that is a **continuous** spectrum of relaxation times could always be used [[12],[8]] . Similarly $\boldsymbol{\sigma}^m$, in eqn. (86), maybe defined by convolution forms involving **fractional derivatives** [[16],[17],[9]], or any **power** type of kernels,

as in [[12],[9],[18]]. Furthermore, it has been demonstrated by Roscoe[19] that, as the number of terms increases, the discrete-spectrum model can approximate any given relaxation/creep function with any desired accuracy, thus obviating the need to further study more complex rheologic models. In addition, very efficient general methods are presently available [e.g., [12] and [20]] to determine **simplified continuous spectra** (i.e., with **small** order or **few** terms that can very well approximate fairly complicated formulae fitted to the experimental data (e.g., creep law's of the power or log-power type) Hence, from both the physical (mechanical-analogs) as well as the **computational** (i.e., **recursive** formulas with **minimal** storage requirements for numerical integration; see section 6 for details) standpoints the **differential models** (and their corresponding exponential-integral- forms, as in eqns. (86-88)), are certainly more appealing for applications..

Remark 1 *As a consequence of the assumed coaxiality of material-moduli tensors* $\mathbf{E}$, $\mathbf{M}$, *and* $\boldsymbol{\eta}$, *the equivalent viscoelastic Poisson's ratio is rendered* **constant** *(i.e., time-independent), thus leading to a neat separation of the characteristic relaxation/retardation times* ρ *and* τ *(see eqns. 86 and 87). Despite the lack of extensive experiments on this specific aspect, there is indication supporting a very small (if any) time-dependent change in Poisson's ratio. In addition, several other arguments in its favor have been also made; e.g., in the solution of boundary-value problems [8]. On the other hand, directly assuming a time-invariant Poisson's ratio is fully consistent with the important theoretical requirement of "***damping-extent ordering***"; i.e., damping in pure shear is larger than in extension, which in turn is larger than damping in bulk, a conclusion that can be reached without any consideration of Poisson's ratio. This is a direct consequence of the "compliance" nature of Poisson's ratio as a material parameter; e.g., implying that the lateral contraction must lag behind the imposed sinusoidally oscillating strain in experiments involving harmonic excitations. This is equivalent to the conclusion that the* **imaginary** *part of the complex, frequency-dependent, Poisson's ratio must be* **negative**; *an issue that has resulted in much controversy in the earlier literature on this subject; e.g., see[[12], [21]]*

Remark 2 *As a corollary to the above remark, one can also introduce material anisotropy; i.e., by simply utilizing the same anisotropic forms for the three tensors* $\mathbf{E}$, $\mathbf{M}$, *and* $\boldsymbol{\eta}$. *All other equations, particularly eqns. (86) and (87) remain unchanged. For example, with transverse isotropy, we have (see [22]) ,where*

$$\mathbf{E} = 2G_l\mathbf{P} - \alpha\mathbf{R} + 2(G_l - G_t)\mathbf{Q} + (\lambda + \frac{\alpha}{3} + \frac{2}{3}G_t)\tilde{\delta}\otimes\tilde{\delta} + [3\alpha + 4(G_l - G_t) + \beta]\tilde{D}\otimes\tilde{D} \quad (89)$$

where

$$\mathbf{P} = \mathbf{I} - \frac{1}{3}\tilde{\delta}\otimes\tilde{\delta}; \qquad \mathbf{I} = I_{ijkl} = \frac{1}{2}(\delta_{ik}\delta_{jl} + \delta_{il}\delta_{jk}) \qquad (89a)$$

$$\mathbf{Q} = Q_{ijkl} = \frac{1}{2}(D_{ik}\delta_{jl} + D_{il}\delta_{jk} + D_{jk}\delta_{il} + D_{jl}\delta_{ik}) - 2D_{ij}D_{kl} \qquad (89b)$$

$$\mathbf{R} = 3\tilde{D} \otimes \tilde{D} - (\tilde{D} \otimes \tilde{\delta} + \tilde{\delta} \otimes \tilde{D}) + \frac{1}{3}\tilde{\delta} \otimes \tilde{\delta} \qquad (89c)$$

with $\tilde{D} = d \otimes d$; d =unit vector defining the "preferred direction" or normal to the plane of isotropy and where $\alpha, \beta, \lambda, G_l$, and G_t are elastic moduli and the symbol $\otimes$ represents a tensor product.

Remark 3 *For many materials, including metals and polymer-based compounds, perhaps the most physically-appealing separation of relaxation mechanisms, according to eqn. (88), is that for viscoelastic deviatoric and purely-elastic volumetric response; i.e., with finite and infinite relaxation times, respectively (τ and ρ in separate "integral" equations for each in eqns. 86 and 87).*

Remark 4 *With a view toward capturing a wider range of temperature a further generalization, providing flexibility for delineating a time dependent and time independent regime (see Fig. 1), would be to explicitly take*

$$\Omega_R = \left\langle \frac{1}{2}\sigma^m_{ij}\eta^{-1}_{ijrs}\sigma^m_{rs} - \Omega_o(T) \right\rangle \qquad (90)$$

where the cut off value is taken as

$$\Omega_o(T) = \frac{1}{2}\sigma^{TI}_{ij}\eta^{-1}_{ijrs}\sigma^{TI}_{rs}$$

The resulting implication would then be reflected by a distinct change in material modulus within the now partitioned quasilinear regime as illustrated in Fig. 6 and eqn. (85).

Remark 5 *It is interesting to note that the same format of* **additive**-*decomposition of "equilibrium-plus-nonequilibrium" stresses and associated energy contributions (Eqns. 19) will remain, even under conditions of large viscoelastic deformations (using second Piola Kirchhoff stresses). This is in conformity with the mathematically consistent and (physically-motivated) approach of* **multiplicative** *split of deformations, that is the deformation gradient tensors (and related "right" Green deformation tensors). Note that under conditions of* **small** *deformations, the latter (multiplicative) decomposition leads directly to its present "***linearized***" form of eqn. 8. For example, see [23] for applications to viscoelasticity; and [24] for alternatives of strain partitioning under more general conditions of large deformation elastoplasticity.*

5.3 Thermodynamic Admissibility; Work and Dissipation Inequalities

When general forms of hereditary convolution representations are utilized, the question of thermodynamic admissibility conditions becomes crucial. This subject has a long standing history in the literature on viscoelasticity [e.g., [8], [9], [25]-[28]]. For example, considering the **one-dimensional** case for simplicity (trivially generalized to the multi-axial case), Rabotnov [9] and Breuer and Onat [25], have formulated the sufficient (but not necessary) condition of positive work; wherein

$$\sigma(t) = \int_0^t \Psi(t-s)\dot{\gamma}(s)ds \tag{91}$$

$$W = \int_0^t \sigma(s)\dot{\gamma}(s)ds \geq 0 \tag{92}$$

and where σ and γ are the one-component (non-equilibrium) stress (see eqn. (87)) and strain field, respectively, and $\Psi(t)$ is a general relaxation kernel. Further conditions involving the nonnegative definiteness and strict monotonicity and convexity of $\Psi(t)$ have been also added:

$$\Psi(s) \geq 0, \quad \Psi'(s) < 0, \tag{93}$$

$$\Psi''(s) \geq 0, \quad \text{for any } s > 0 \tag{94}$$

These are typically derived by considering step-loading strain functions. However, in order to define a complete set of conditions on $\Psi(t)$ a more comprehensive set of conceived loading programs should be utilized; i.e., a sequence of many constant-strain steps of alternating signs, occurring at times $t = 0, h, 2h, ..., nh$ in the limit $h \to 0$, thus leading to the use of the theory of distributions [[29], [30]] for generalized/singularity loading functions (delta, dipole, ... functions) $\dot{\gamma}_n(s) = \delta^{(n)} = \frac{d^n\delta}{ds^n}$ (see Fig. 7 for an illustration). Together with the requirement of **fading memory**, it can be shown that this leads to more conditions of the type

$$(-1)^n \frac{d^n\Psi(s)}{ds^n} \geq 0, \qquad s > 0, \qquad n = 0, 1, 2... \tag{95}$$

The above condition is simply derived as follows. With $\dot{\gamma} = \delta^{(n)}$,the first of eqn. (92) gives $\sigma(t) = \Psi^{(n)}(t)$, whose sign must then be matched to that dictated by the fading-memory assumption. To this end, and depending on whether "n" is even (or odd), we note that a strain-rate history $\dot{\gamma}(s) = \delta^{(n)}(s)$ is expected to give, for $t > nh$ (in the limit $h \to 0$), a nonnegative (nonpositive) stress response, in accordance with a fading memory hypothesis for a strain-rate history having identical (in magnitude, but **opposite** signs) changes, with the more recent being positive (or negative). In their present form, the above conditions (eqns. (95)) define a **completely monotonic function**. Although this excludes some of the nonstandard relaxation functions (e.g., used in instability studies of

shockwave fronts in viscoelastic composites [[28],[31]]), the above conditions will eliminate any physically unrealistic representations, such as "negative" viscosity in the equivalent mechanical analog of series of springs/dashpots [27]. It is important to note that utilizing the internal-variable formalism, i.e., with the complementary energy and dissipation rate functions discussed herein, all of the above conditions are automatically satisfied once the positive-definiteness and non-negativeness of the elastic (E_{ijkl}, M_{ijkl}) and viscosity (η_{ijkl}) moduli are ensured, respectively.

As an alternative to the above derivation, a more rigorous mathematical approach can be utilized here. Its formal setting is that for functional analysis of the problem of evolution with linear operators using the **semigroup** theory (e.g., [32]). For the present case, the semigroup corresponds to the convolution operator, $T_{t+s} = T_t \circ T_s$ for mapping composition,with $\{T_t\dot{\gamma} = (\Psi * \dot{\gamma})(t)\}, t \geq 0$, where "$*$" indicates convolution, and subscript and argument "t" indicate the parameter for this one-parameter family {} of continuous linear operators. Aside from a number of technical conditions that are standard in the literature of semigroup theory, there are two important conditions here. The first stems from the existence of the natural, **nonnegative**, semi-norm induced by the associated inner product; i.e., here this corresponds to the **positive** work condition in eqn. (92)

$$W =< T_t\dot{\gamma}, \dot{\gamma} >=< \sigma, \dot{\gamma} >= \int_0^t \sigma(s)\dot{\gamma}(s)ds \geq 0 \tag{96}$$

Using the history $\dot{\gamma}(s) = \delta^{(n)}(s)$, and carefully accounting for the singularity of $\delta^{(n)}(s)$ in calculating the inner product, we use ($\sigma(s) = \Psi^{(n)}$)

$$W =< \sigma, \dot{\gamma} >= (\Psi^{(n)} * \dot{\gamma})(0)$$

or

$$W = (\Psi^{(n)} * \hat{\delta}^{(n)})(0) = (-1)^{2n}\Psi^{(2n)}(0) \geq 0 \tag{97}$$

where $\hat{\delta}(s) = \delta(-s) = \delta(s)$ = reflexive mapping of Dirac's distribution or $\delta-$ function, and (0) indicates functions evaluated at t=0. Generalization from initial (zero) to any fixed (time a) time is trivial, through the convolution translation rule $(\Psi * \delta)(s-a) = (\Psi(s) * \delta(s-a))$. Thus we get from (97), for any general time t,

$$(-1)^{2n}\Psi^{(2n)}(t) \geq 0 \qquad t \geq 0 \tag{98}$$

Following a similar procedure, the second condition, pertaining to the **dissipativity** (contractivity) of the associated infinitesimal generator [32], here reduced simply to the **dissipation inequality**, e.g., see Ω_V, in eqn. (9):

$$\begin{aligned} \Omega_V &= - < \dot{\gamma}, D_t T_t \dot{\gamma} > \\ &= -(\dot{\gamma} * \dot{\sigma})(0) \\ &= -(\delta^{(n)} * \frac{d\Psi}{dt} * \tilde{\delta}^{(n)})(0) \end{aligned}$$

or using convolution-time-shift properties

$$\Omega_V = -\Psi^{(2n+1)}(t) \geq 0 \tag{99}$$

for any t $\geq$ 0.

The above conditions in (98) and (99) were obtained under very general conditions; they are applicable irrespective of the extent or type of material memory implied by the use of general kernels in eqns. (86) and (87). Remarkably, they have combined to give exactly the same conditions of the nonnegative (or nonpositive) characteristics for even (or odd) order time derivatives of the kernel functions.

Remark 6 *Starting from the additive decomposition for stress in eqn. (26), one can then adopt any general kernel in the equation defining the integral form of the nonequilibrium stress, σ^m (see eqn. (87)), and proceed to use the constraint eqns. (98) and (99), with σ^m and $\dot{e}$ replacing σ and $\dot{\delta}$, respectively, as formal definitions for the stored energy (the complementary Gibb's function follows through a conventional Legendre transformation) and viscous dissipation function, respectively. This has two main advantages. Firstly, the direct definition, specially for the stored energy, will alleviate the well-known difficulties that may arise in attempting to derive them using alternative approaches (often with further assumptions), e.g., see [[8],[9]]. Secondly, satisfying the shown inequalities in eqns. (98) and (99) will also automatically ensure thermodynamic admissibility.*

Remark 7 *In conjunction with the previous remark, and generalizing to multiaxial cases, i.e., with $e(s) = \delta^{(n)}(s)e_o$ where e_o is the fixed "strain-direction" tensors. We further need the positive (semi) definiteness of tensors* $\mathbf{E}$, $\mathbf{M}$, $\boldsymbol{\eta}$ *(in addition to eqns. (98) and (99)) for full compliance with the thermodynamic admissibility conditions.*

6 Recursive Algorithm For Numerical Integration

Considering the internal variables, the key aspect in the formulation of discrete time stepping procedures concerns the evaluation of the convolution integral in eqn.(86). In the present context, and utilizing the **strain-driven** form in eqn.(87), as typical in finite-element computations, the crucial observation is that the following recursive relation holds, for advancing the solution from step t_n to t_{n+1} with $\Delta t = t_{n+1} - t_n$:

$$\begin{aligned}
\boldsymbol{\sigma}^m_{n+1} &= \int_0^{t_{n+1}} e^{-\frac{(t_n+\Delta t-s)}{\rho}} \frac{d}{ds}[\boldsymbol{\eta}^* \mathbf{e}]ds \\
&= \int_0^{t_n} e^{-\frac{(t_n+\Delta t-s)}{\rho}} \frac{d}{ds}[\boldsymbol{\eta}^* \mathbf{e}]ds + \int_{t_n}^{t_{n+1}} e^{-\frac{(t_{n+1}-s)}{\rho}} \frac{d}{ds}[\boldsymbol{\eta}^* \mathbf{e}]ds
\end{aligned}$$

or

$$\boldsymbol{\sigma}_{n+1}^{m} = e^{-\frac{(\Delta t)}{\rho}}\boldsymbol{\sigma}_{n}^{m} + e^{\frac{-(\Delta t)}{2\rho}}\boldsymbol{\eta}^{*}\boldsymbol{\Delta e} \tag{100}$$

where $\Delta e = e_{n+1} - e_n$ is the given strain increment in the step. In the second term of eqn.(100), the **midpoint rule**, known for its second-order accuracy[[33],[34]] has been used to linearly approximate the derivative.

Note that the above algorithm requires the values of $\boldsymbol{\sigma}_{n}^{m}$ as the **only** historical data to be stored. Also, that this scheme provides for **unconditionally stable**[[33],[34],[35]] time stepping as well as the correct limits for large and vanishingly small times.

7 Parametric Study

Here we will utilize eqns.(54) and (56) to conduct creep parametric studies to study the influence of the various material parameters with an eye toward providing guidance and insight into the experimental characterization of the proposed model. Basically six material parameters will be assessed, i.e., E_s,E_m,E_η, ν_s, ν_m, and ν_η; however, in keeping with our previous discussion (see eqns. (86) and (87)) E_m and E_η will be studied in the context of their respective material time clocks (i.e., relaxation and creep (retardation) times) $\rho\mathbf{I} = \mathbf{M}^{-1}\boldsymbol{\eta}$ and $\tau\mathbf{I} = \overline{\mathbf{EM}}^{-1}\boldsymbol{\eta}$, respectively, and their ratio $\alpha\mathbf{I} = (\frac{\tau}{\rho}-1)\mathbf{I} = \mathbf{E}^{-1}\mathbf{M}$. Such a reduction can be accomplished only if we assume all Poisson's ratios to be equal, i.e., $\nu = \nu_s = \nu_m = \nu_\eta$, and then take the ratio of the various moduli tensors as indicated above. In this way, eqns. (69) and (70) are reduced, such that in the case of uniaxial creep $\mathbf{X}$ and $\mathbf{Y}$ become:

$$\mathbf{X} = \sigma^{*}(1 - (\frac{\alpha\rho}{\tau})e^{-\frac{t}{\tau}})\begin{bmatrix} 1 \\ 0 \\ 0 \end{bmatrix} \tag{101}$$

$$\mathbf{Y} = \frac{\sigma^{*}}{E_s}(1 - (\frac{\alpha\rho}{\tau})e^{-\frac{t}{\tau}})\begin{bmatrix} 1 \\ -\nu \\ -\nu \end{bmatrix} \tag{102}$$

and the parametric study is reduced to the investigation of only four independent parameters, that is, E_s (or E), τ, ρ, and ν. In all creep test simulations the load (stress) was applied along the 11 direction, at a rate of 0.5 ksi/sec, to a constant level of 1 ksi and than held fixed for a given duration of typically 10τ. The parametric study begins with the influence of one's choice for the various Poisson's ratios and is then followed by the effect of the infinite elastic stiffness (E_s), the influence of the stiffness of the dashpot (viscous) element relative to the nonviscous stiffnesses (i.e., τ), and then lastly the influence of the viscous to the nonviscous stiffness within the Maxwell element itself (i.e., ρ). Note that the variations of these parameters can be interpreted as simulating the behavior of the model over a given temperature range, as this would be a mechanism that could cause such a perturbation in the various moduli and Poisson's ratios.

7.1 Effect of Poisson's Ratios

It is important to note that even with the restrictions to isotropy and uniaxial loading there remain in the general forms of eqns. (70) significant triaxiality and interaction effects among the various internal stress and strain components for nonzero and distinct Poisson's ratios of the different elastic and viscous elements. To investigate this interaction behavior, we examined the seven cases given in Table 1, where the stiffness values were fixed at base line values (assumed based on Fig. 2b of Part II [10]) while the values of the Poisson's ratios were changed.

Table 1 Material parameters used for results generated in Figs. 8-18.

Case	E_s (ksi)	E_m (ksi)	ρ (sec)	E_η (ksi-sec)	τ (sec)	ν_s	ν_m	ν_η
1	8500.	8500.	333.35	2833475.	666.7	0	0	0
2	"	"	"	"	"	0.2	0.2	0.2
3	"	"	"	"	"	0.3	0.3	0.3
4	"	"	"	"	"	0.4	0.4	0.4
5	"	"	"	"	"	0.49	0.3	0.3
6	"	"	"	"	"	0.3	0.3	0.49
7	"	"	"	"	"	0.3	0.49	0.49

The creep results for cases 1 through 4 are shown in Figs. 8-12, where Fig. 8 shows the stress versus strain, Figs. 9 and 10 the 11- and 22-strain versus time history, Figs. 11 the equilibrium stress (stress in the spring element) in the 11 direction versus time, and finally Fig. 12 the effective overall Poisson's ratio versus time. Examining these figures and eqns. (101) and (102), it is clear that when the individual Poisson's ratios are all equal:

- The stress versus strain behavior is unaffected, irrespective of the value of Poisson's ratio taken, as is the strain in the 11 direction and the equilibrium stress in all directions.
- The 22 (shown here) and 33 strain component is, as expected, highly influenced by the value of the Poisson's ratio chosen.
- Only primary creep response is generated, with this transient period ending after **approximately** 7τ, when the equilibrium stress in the loading direction becomes equal to the applied stress in that direction, i.e., the elastic limit of the material is reached.
- The equilibrium stress in the transverse directions are zero, as expected given that the material is homogenous and the applied stress in those directions are zero.
- The effective Poisson's ratio is **independent of time** and equal to the Poisson's ratios of the individual elements.

Considering three additional cases (i.e., cases 5, 6,and 7, respectively) in which, 1) the single spring element is taken to be purely deviatoric, 2) the viscous element in the Maxwell element is deviatoric and 3) the entire Maxwell element is taken to be purely deviatoric (i.e., $\nu_m = \nu_\eta \approx 0.5$). Note that in these cases the material is, in essence, implicitly assumed to be inhomogeneous. Consequently, the specialized uniaxial forms in eqns. (101) and (102) are not applicable and the more complex but general eqns.(69) and (70) must be used. The results for cases 1, 5, 6 and 7 of Table 1 are shown in Figs. 13 through 18. Examining these figures one immediately sees that if the Poisson's ratios are not all taken equal to one another:

- The initial effective stiffness can be increased (see Fig. 13).
- The time required to reach the elastic limit can increase to as much as 100τ, as there is likely to be more than a single internal clock present (see G^* and K^*).
- Although the total accumulated 11 strain, and 11 and 22 equilibrium stress components are the same as before, the transient portions are highly influenced by the assumed value of the various Poisson's ratios. In particular note the difference in the sign of the equilibrium stress in the 22 direction for case 5 as compared with cases 6 and 7. (see Figs. 14, 16 and 17)
- The effective Poisson's ratio becomes time dependent for the cases when the individual element Poisson's ratios are not the same. With the initial effective ratio being equal to that given in eqn. (78) and the final being that of the single spring element (i.e., ν_s). This observation provides us with insight into the needed critical test to characterize, as well as validate, the present model construction. (see Fig. 18)

Obviously, this demonstrates the rather limited usefulness of one-dimensional modeling and fitting in realistic representations for general applications. In fact, any ad-hoc extrapolation assumptions made [e.g., [11] or [36]] can lead to rather erratic history predictions of the implied Poisson's-effect history (i.e., time intervals of alternating negative and positive Poisson's ratios). Apparently the difficulty stems from the complex dependency of both the transverse as well as the axial strain components on the three coupled Poisson's factors, thus rendering it extremely difficult to define a simple operator form (creep compliance/ relaxation modulus) for their ratios as would be the case in these simple ad-hoc extrapolation schemes. Such difficulties and anomalous predictions can of course be completely by-passed provided the **coaxiality** of **all** elastic moduli tensors are imposed and the conventional engineering material parameter bounds, i.e., positive moduli and $0 \leq \nu_i \leq 0.5$ are adhered to in our general formulation (ensuring the convexity of the two complementary potentials under study). This coaxiality assumption appears to be experimentally justifiable at this time, as preliminary measurements (see Part II, [10]) have indicated that the effective Poisson's ratio is time independent.

7.2 Effect of Infinite Elastic Stiffness, E_s

Next, four cases were examined in which the infinite elastic stiffness (i.e., that of the lone spring element, in Fig. 4a) was varied from 2000 to 12500 ksi as identified in Table 2. Note that in these cases, as in the previous seven, the spring stiffness (E_s) is taken equal to that of the spring stiffness within the Maxwell element (i.e., E_m), that is the ratio $\alpha = 1$. Results are presented in Figs. 19, and 20, where the resulting stress versus strain history and strain versus

Table 2 Material parameters used for results in Figs. 19-20.

Case	E_s (ksi)	E_m (ksi)	ρ (sec)	E_η (ksi-sec)	τ (sec)	ν_s	ν_m	ν_η
1	2000.	2000.	333.35	666700.	666.7	0.3	0.3	0.3
2	4500	4500	"	1500075.	"	0.3	0.3	0.3
3	8500	8500	"	2833475.	"	0.3	0.3	0.3
4	12500	12500	"	4166875.	"	0.3	0.3	0.3

time history are shown. Figures 19 and 20 clearly indicate, as one might expect from eqn. (102), that the effective load-up stiffness is strongly influenced (increased) and the accumulation of time-dependent strain is also highly influenced (decreased) by increasing the assumed value of E_s. Such a result is necessitated by our insistence upon maintaining a constant ρ, τ and α ratio. Similarly, the resulting equilibrium stress versus time history and effective Poisson's ratio history are identical with those described in Figs. 11 and 12, respectively, and the total accumulated transverse strains are clearly just the opposite of those shown in Fig. 20 with the magnitude being scaled by the Poisson's ratio (see eqn. (102)). As an aside, the trends observed in Figs. 19 and 20 are in keeping with those one might expect as they decreased the temperature of the material.

7.3 Effect of Varying the Characteristic Creep (Retardation) Time, τ

Now we consider four cases which illustrate the influence of τ on the creep response of the material, wherein all other parameters are fixed at the base line values. As τ is a ratio ($\overline{EM}^{-1}\eta$) and we desire that ρ remain constant, E_m, must therefore be modified. The four sets of material parameters used are given in Table 3. Note that by necessity α is equal to 0.1, 1, 2, and 5 for cases 1, 2, 3, and 4, respectively.

Table 3 Material parameters used for results in Figs. 21-22.

Case	E_s (ksi)	E_m (ksi)	ρ (sec)	E_η (ksi-sec)	τ (sec)	ν_s	ν_m	ν_η
1	8500.	850.	333.35	283347.5	366.7	0.3	0.3	0.3
2	8500	8500	"	2833475.	666.7	0.3	0.3	0.3
3	8500	17000	"	5666350.	1000.	0.3	0.3	0.3
4	8500	42500	"	14167375.	2000.	0.3	0.3	0.3

The resulting stress-strain and strain-time(and equilibrium stress (X, σ_s) versus time) response histories are shown in Figs. 21 and 22, respectively. Examining eqn. (102) and Fig. 21, it is clear that the effective load-up modulus is once again increased as E_m (or correspondingly α) and τ are increased, however, this time the total accumulated strain remains the same in all cases; as the elastic limit strain ($\frac{\sigma^*}{E_s}$) remains fixed, i.e., E_s = 8500 ksi. This is opposite to the cases in Fig. 19, where E_s is continuously being increased and thus the elastic limit strain is being reduced in each case. *Consequently, one has sufficient freedom in this model to modify the effective load-up modulus without correspondingly reducing the total amount of strain accumulation.* Figure 22 and eqn. (102) again, clearly indicate another influence of increasing τ, that is, to increase the duration of the primary (transient) zone of the time-dependent straining. Note that in all cases the primary zone is complete (with respect to the external clock) by approximately 7 times the associated internal clock (i.e., τ). This fact can be extremely helpful in characterizing the proposed model, in that we can deduce the internal clock from the experimentally observed saturation time (external clock). Similarly, if we experimentally observe that the saturation time of primary creep is independent of temperature, one would conclude that τ should also be taken to be temperature independent. Lastly, as the individual Poisson's ratios are all equal, the effective Poisson's ratio is time independent (see Fig. 12) and the 22 and 33 components of total strain are simply appropriately modified mirror images of the 11 component, and the 22 and 33 equilibrium stresses are zero (see eqn. (102)).

7.4 Effect of Varying the Characteristic Relaxation Time, ρ

Finally, we will consider four cases which illustrate the influence of ρ on the creep response of the material, wherein all other parameters are fixed at the base line values. Once again, as ρ is a ratio ($\mathbf{M}^{-1}\boldsymbol{\eta}$) and we desire that τ and α remain the same as in the previous cases, i.e., τ = 666.7 and $\alpha = 0.1, 1, 2,$ and 5 ; $\boldsymbol{\eta}$, must therefore be modified. The four sets of material parameters used to generate Fig. 23 are given in Table 4.

Table 4 Material parameters used for results in Figs. 23-26.

Case	E_s (ksi)	E_m (ksi)	ρ (sec)	E_η (ksi-sec)	τ (sec)	ν_s	ν_m	ν_η
1	8500.	850.	606.09	515176.5	666.7	0.3	0.3	0.3
2	8500	8500	333.35	2833475.	"	0.3	0.3	0.3
3	8500	17000	222.23	3777910.	"	0.3	0.3	0.3
4	8500	42500	111.12	4722600.	"	0.3	0.3	0.3

Here the resulting stress-strain history is identical to that of Fig. 21, as both E_s and E_m are the same as in the previous cases. The strain-time and equilibrium stress versus time histories are influenced however, as one might suspect, for example see Fig. 23. Comparing Figs. 23 to 22, we see no influence of ρ on the duration of the primary creep regime, as one would expect given eqn. (102). However, the rate of accumulation is

slightly influenced, given the same value of α, as seen in Fig. 23. Clearly, in relaxation ρ would now have a significant influence on the duration of stress relaxation.

Revisiting the influence of the individual Poisson's ratios, we re-examine the cases in Table 4, but this time we take $\nu_s = 0.1$ while $\nu_m = \nu_\eta = 0.3$. Again, the stress-strain history is identical and the 11 component histories of the total strain and equilibrium stress are very similar, the duration of the transient zone just being extended. The 22 components, however, become highly time dependent as does the effective Poisson's ratio of the material model. These response histories are illustrated in Figs. 24-26, respectively. Note that the behavior of the components transverse to the load are quite complex, and again the only sure way to validate the model assumptions is to collect experimental data in those directions.

8 Conclusions

Traditionally, the total strain has been partitioned into elastic (time-independent reversible), inelastic (irreversible) and thermal (reversible) strain components, where the inelastic strain corresponds to such physical phenomena as time-independent plastic strain or time-dependent viscoplastic strain (sometimes referred to as creep strain). In this paper alternative forms for the hereditary integrated representations of the viscoelastic response were discussed to account for the time/rate dependent reversibility typically observed in experiments on materials exhibiting quasilinear domains. This discussion was in the context of a general framework for the viscoelastoplastic material modeling of the internal-state-variable type. It was shown that such a potential based framework necessitated the specific partitioning of **both** the strain (reversible and irreversible) and stress (equilibrium and non-equilibrium) state variables. Important key issues, pertaining to both the theoretical foundation (e.g., thermodynamic admissibility) as well as the numerical implementation (e.g., recursive integral forms) of these general descriptions were discussed. In particular, explicit constraints on the underlying kernel functions were given. Furthermore, even though numerous multiaxial formulations have been noted in the literature in their symbolic form, it was demonstrated here that without the assumption of **equal** Poisson's ratios (**coaxiality** of the various moduli tensors) the uniaxial reduction to the classical linear solid element, is **not** possible given the starting viewpoint of internal state variables, defined through either the differential or convolution integral approach. Of course, as implied by classical forms, taking all Poisson's ratios to be **zero** is merely a **special** case of this **equality** condition.

Several parametric studies and qualitative response assessments were made to help identify important factors in the actual characterization of the specific-form of the model studied for the titanium alloy, **TIMETAL 21S**, as discussed in Part II [10]. The more important, with respect to characterization, parametric results are itemized as follows:

- If the experimentally observed effective Poisson's ratio is **independent of time** then all individual mechanical elements' Poisson's ratios can be assumed equal

to that of the measured one, thereby significantly reducing the complexity of the required reversible constitutive model. Several other considerations (e.g., damping-extent ordering) were also found to favorably support this assumption.

- Only primary creep response is generated, with this transient period ending after **approximately** 7τ (given the assumption of equal Poisson's ratios), when the equilibrium stress in the loading direction becomes equal to the applied stress in that direction, i.e., the elastic limit of the material is reached. Consequently, τ , the internal material clock, can be immediately obtained by dividing the experimentally observed saturation time by seven. However, this is not the case when different Poisson's ratios are assumed wherein the period now intricately depends upon these ratios (and the "implied" number of internal clocks are increased).

- The effective load-up stiffness is strongly influenced (increased) and the accumulation of time-dependent strain is also highly influenced (decreased) by increasing the assumed value of E_s. Consequently, variation with temperature of E_s should be a key factor under nonisothermal conditions.

- If the assumption of constant Poisson's ratios is accurate, than eqn. (79) proves that the dynamic modulus is equal to the sum of E_s and E_m, i.e., $E_0 = E_s + E_m$, and E_m can be deduced from directly measurable quantities.

- One has **sufficient** freedom in this model to modify the effective load-up modulus without correspondingly reducing the total amount of strain accumulation. Increasing τ increases the duration of the primary (transient) zone of the time-dependent straining. Similarly, if we experimentally observe that the saturation time of primary creep is independent of temperature, this would than imply that τ should also be taken to be temperature independent.

Armed with these insights, and assuming the validating of a time-independent effective Poisson's ratio the characterization of the proposed multiaxial reversible model is straight forward. Alternatively, if the effective Poisson's ratios are time dependent, then one may need the assistance of an automated material parameter estimator, [37], as would be necessarily the case for a wider relaxation mechanism spectrum (greater frequency-dependency of the moduli) calling for several internal state variables. The companion paper (see Part II [10]) will focus on the actual characterization and comparison with test results for a model material, i.e., **TIMETAL 21S**, over a wide range of temperatures (i.e., 23 to 650 °C).

Finally, given the host of viscous effects present in structural applications at elevated temperatures, the practical utility of such a generalized hereditary form as presented herein is significant. For example considering that most aerospace engine designs are typically limited to the quasilinear stress and strain regimes, as in this case the reversible time-dependent response component becomes dominate in comparison to the irreversible component. Alternatively, one can envision another extreme case (e.g., in polymer and

rubber based systems under varying temperatures) in which a purely reversible viscous response is present, thus necessitating the use of such a theory. And lastly, an obvious natural extension for general applicability is the middle ground in which a combined reversible and irreversible representation is required. Here the inclusion of a reversible time-dependent response as that discussed in this paper will extend the applicable predictive stress and/or temperature window of application.

References

[1] Arnold, S.M.; and Saleeb, A.F.: On the Thermodynamic Framework of Generalized Coupled Thermoelastic Viscoplastic - Damage Modeling. , Int. Jnl. Plasticity, Vol. 10, No. 3, 1994, pp. 263-278, or NASA TM-105349, 1991.

[2] Arnold, S.M., Saleeb, A.F, and Wilt, T.E.: A Modeling Investigation of Thermal and Strain Induced Recovery and Nonlinear Hardening in Potential Based Viscoplasticity, Jnl. of Engng. Materials and Technology, Vol. 117, No.2, 1995, pp. 157-167, or NASA TM-106122, 1993.

[3] Lubliner, J., "On the Thermodynamic Foundations of Nonlinear Solid Mechanics," Int. J.. Nonlinear Mech., Vol. 7, 1972, pp. 728

[4] Lemaitre, J.; and Chaboche, J.L.: *Mechanics of Solid Materials*, Cambridge University. Press, New York, 1990.

[5] Truesdell, C., and Noll, W., The Nonlinear Field Theories, in Handbook of Physics, Vol. III/3, (S. Flugge, editor), Springer, Berlin, 1965.

[6] Arnold, S.M.; Saleeb, A.F., and Castelli, M.G.: A Fully Associative, Nonlinear Kinematic, Unified Viscoplastic Model for Titanium Based Matrices, *Life Prediction Methodology for Titanium Matrix Composites*, ASTM STP 1253, W.S. Johnson, J.M. Larsen, and B.N. Cox, Eds., 1996, or NASA TM-106609, 1994.

[7] Arnold, S.M.; Saleeb, A.F., and Castelli, M.G.: A Fully Associative, Nonisothermal, Nonlinear Kinematic, Unified Viscoplastic Model for Titanium Based Matrices, *Thermomechanical Fatigue Behavior of Materials: Second Volume*, ASTM STP 1263, M.J. Verrilli and M.G. Castelli, Eds., Philadelphia,1995, or NASA TM-106926, 1994.

[8] Christensen, R., *Theory of Viscoelasticity*, Academic Press, New York, 1971.

[9] Rabotnov, Y.N., *Elements of Hereditary Solid Mechanics*, Mir Publishers, Moscow, 1980.

[10] Arnold, S.M.,Saleeb, A.F. and Castelli, M.G. : A General Reversible Hereditary Constitutive Model: Part II: Application to A Titanium Alloy, submitted to Int. J. Solids and Structures, or NASA TM 107494, 1997.

[11] Flügge W., *Viscoelasticity*, Second Revised Ed., Springer Verlag, New York, 1975

[12] Tschoegl, N.W., *The Phenomenological Theory of Linear Viscoelastic Behavior*, Springer-Verlag, Berlin, 1989.

[13] Majors, P.S. and Krempl, E., "Recovery of State Formulation for Viscoplasticity Theory Based on Overstress", High Temperature Constitutive Modeling and Application, Freed, A.D. and Walker, K.P., Eds., ASME, AMD Vol. 121, 1991, pp. 235-250.

[14] Onat, E.T., and Fardshisheh, F., Representation of Creep of Metals, ORNL TM-4783, Oak Ridge National Laboratory, Oak Ridge, TN, 1972.

[15] Miller, A.K., *Unified Constitutive Equations For Creep and Plasticity*, Elsevier Applied Science,1987.

[16] Bagley, R.L. and Torvik, P.J., Fractional Calculus- A Different Approach to the Analysis of Viscoelastically Damped Structures, AIAA Journal, Vol. 21, No. 5, 1983, pp. 741-748.

[17] Koeller, R.C., Application of Fractal Calculus to the Theory of Viscoelasticity, J. Appl. Mech., Vol. 51, No. 2, 1984, pp. 299-307.

[18] Leaderman, H., Elastic Properties of Filamentous Materials, The Textile Foundation, Washington, D.C., 1943.

[19] Roscoe, R, Mechanical Models for Representation of Viscoelastic Properties, British J. of Applied Physics, Vol. 1, 1950, pp. 171-173.

[20] Matteo, C.L. and Cerveny S., A Nonlinear Method for Calculation of the Loss Tangent Distribution Function, Rheologica Acta, Vol. 35, 1996, pp. 315-320.

[21] Waterman, H. A., "Relations Between Loss Angles in Isotropic Linear Viscoelastic Materials", Rheologica Acta, Vol. 16, 1977, pp. 31-42.

[22] Saleeb, A.F. and Wilt, T.E., "Analysis of the Anisotropic Viscoplastic-Damage Response of Composite Laminates - Continuum Basis and Computational Algorithms", Int. J. Num. Meth. Eng., Vol. 36, 1993, pp. 1629-1660.

[23] Lubliner, J. "A Model of Rubber Viscoelasticity," Mechanics Research Comm., Vol. 12, 1985, pp. 93-99.

[24] Nemat-Nasser, S., "Decomposition of Strain Measures and Their Rates in Finite Deformation Elastoplasticity", Int. J. Solids and Structures, Vol. 15, 1979, pp. 155-166.

[25] Breuer, S. and Onat E., On Uniqueness in Linear Viscoelasticity, Quarterly of Appl. Mech., Vol. XIX(4), 1962, pp. 355-359.

[26] Rivera, J.E., Asymptotic Behavior in Linear Viscoelasticity, Quarterly of Appl. Math., Vol. LII, No. 4, 1994, pp. 629-648.

[27] Akyildis, F, Jones, R.S., and Walters, K., On the Spring-Dashpot Representation of Linear Viscoelastic Behavior, Rheologica Acta, Vol. 29, 1990, pp. 482-484.

[28] Hazanov, S., On One Dynamic Model for Composite Materials, in Constitutive Laws for Engineering Materials (C. Desai et al, Eds.), ASME Press, Tucson, AZ, 1991, pp. 275-278.

[29] Lighthill, M.J., *Introduction to Fourier Analysis and Generalized Functions*, Cambridge University Press, Cambridge, 1958.

[30] Friedlander, F.G., *Introduction to the Theory of Distributions*, Cambridge University Press, Cambridge, 1982.

[31] Starr, P. V., *Physics of Negative Viscosity Phenomena*, McGraw Hill, New York, 1968.

[32] Pazy, A., Semigroups of Linear Operators and Applications to Partial Differential Equations, Appl. Math Science, Vol. 44, Springer-Verlag, New York, 1983.

[33] Richtmyer, R.D., and Morton, K.W., *Difference Methods for Initial Value Problems*, 2nd edition, John-Wiley, NY, 1967.

[34] Gear, C.W., *Numerical Initial Value Problems in Ordinary Differential Equations*, Prentice Hall, Englewood Cliffs, 1971.

[35] Fortin, M., and Glowinski, R., *Augmented Lagrangian Methods: Application to the Numerical Solution of Boundary-Value Problems*, North-Holland, Amsterdam, 1983.

[36] Shames, I.H. and Cozzarelli, F.A., Elastic and Inelastic Stress Analysis, Prentice Hall, Englewood Cliffs, NJ, 1992.

[37] Saleeb, A.F., Gendy, A.S., and Wilt, T.E., Parameter Estimation for Viscoplastic Material Modeling", NASA TM, 1997.

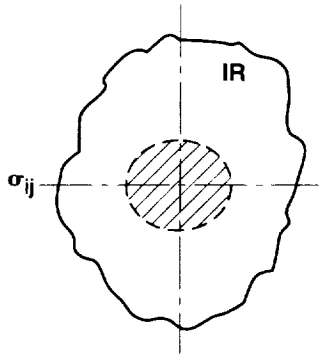

(a) High temperature.

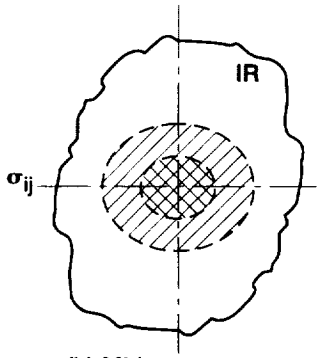

(b) Mid temperature.

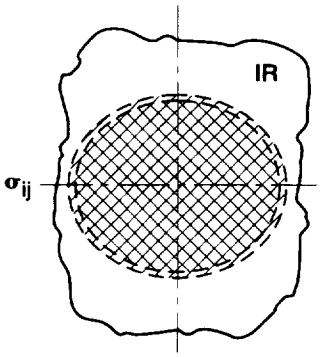

(c) Low temperature.

Time independent reversible region

Time dependent reversible region

IR Irreversible (quasilinear) region

Fig 1.—Reversible and irreversible threshold surfaces.

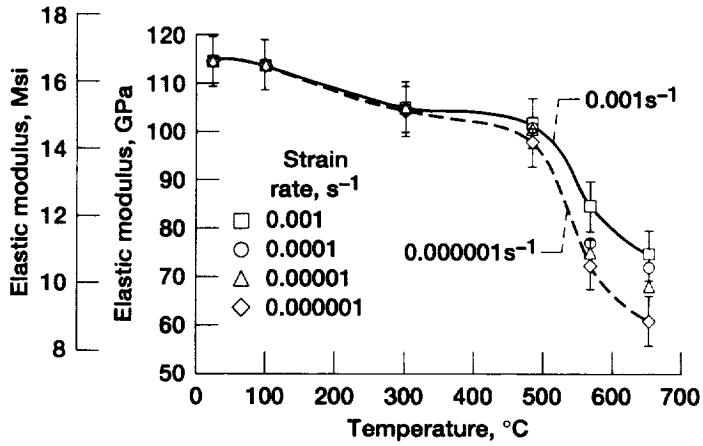

Fig 2.—Rate sensitivity of static stiffness, timetal 21S.

Partitioning the strain

$$\dot{e} = \dot{e}^e + \dot{\epsilon}^I$$

$$\dot{e} = \frac{\dot{\sigma}}{E_1} + \dot{\epsilon}^I$$

$$\dot{\epsilon}^I = \frac{(\sigma-\alpha)^n}{\eta_3}$$

$$\dot{\alpha} = E_2\left[\dot{\epsilon}^I - \frac{\alpha^m}{\eta_2}\right]$$

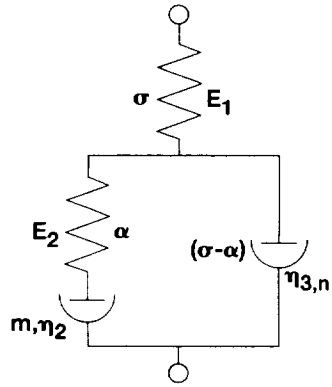

(a) Generalized four element: viscoplastic.

Partitioning the strain

$$\dot{e} = \dot{e}^e + \dot{\epsilon}^c$$

$$\dot{e} = \frac{\dot{\sigma}}{E_0} + \dot{\epsilon}^c$$

$$\dot{\epsilon}^c = \dot{\epsilon}^p + \dot{\epsilon}^s$$

$$\dot{\epsilon}^p = \frac{(\sigma-\alpha)^n}{\eta_2}$$

$$\dot{\epsilon}^s = \frac{\sigma^m}{\eta_4}$$

$$\dot{\alpha} = E_1\left[\dot{e} - \frac{\sigma^m}{\eta_4}\right]$$

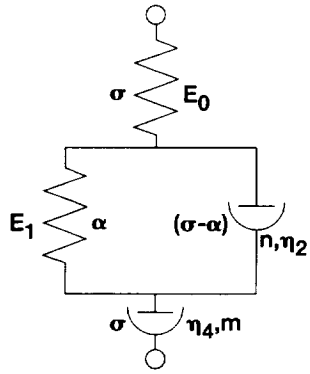

(b) Classic four element: viscoelastic.

Fig 3.—Four element mechanical models depicting the deformation response of a material.

Partitioning the stress

$$\sigma = \sigma_s + \sigma_m$$

$$e^{ve} = \frac{1}{E_s}(\sigma_s)$$

$$\dot{\sigma}_s = \frac{E_m E_s}{EM}\left[\frac{\dot{\sigma}}{E_m} + \frac{(\sigma-\sigma_s)^n}{\eta}\right]$$

$$EM = E_s + E_m$$

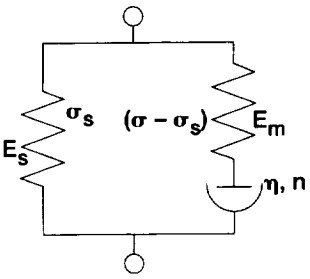

(a) Generalized standard solid.

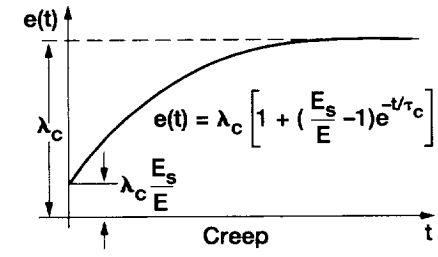

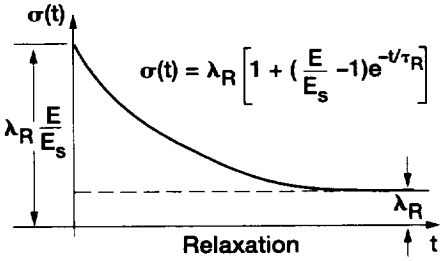

	λ_c	τ_c	λ_R	τ_R
Three element (Fig 3b)	$\frac{\sigma_0 E}{E_m E_s}$	$\frac{\eta}{E_s}$	$\frac{\sigma_0 E_s}{E}$	$\frac{\eta}{E}$
Standard linear (Fig 4a)	$\frac{\sigma_0}{E_s}$	$\frac{\eta E}{E_m E_s}$	$\frac{\sigma_0 E_s}{E}$	$\frac{\eta}{E_m}$

$E = E_s + E_m$

(b) Solution response.

Fig 4.—Three element mechanical model and corresponding creep and relaxation response history.

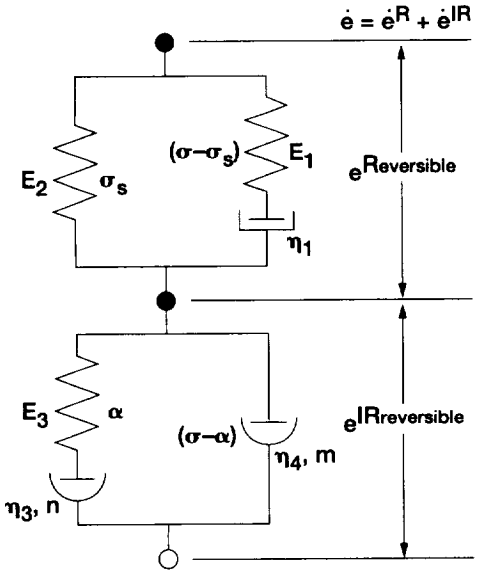

Fig 5.—General hereditary behavior model indicated with appropriate partitioning of stress and strain.

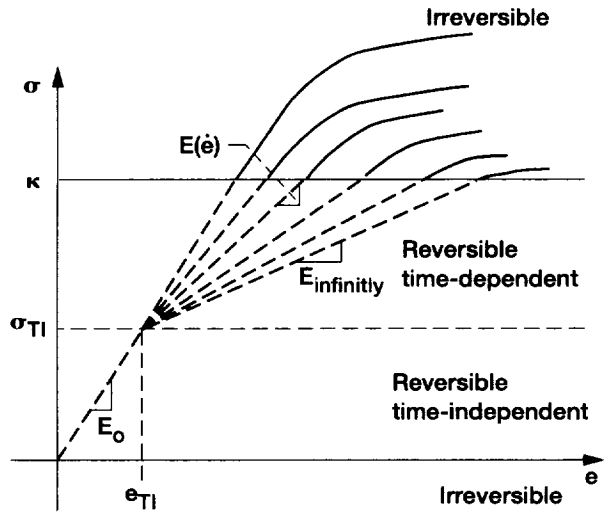

$$e^R = E_o^{-1}\,\sigma_{TI}(T) + E_\infty^{-1}\langle\sigma-\sigma_{TI}(T)\rangle$$

Fig 6.—Uniaxial depiction of reversible and irreversible domains.

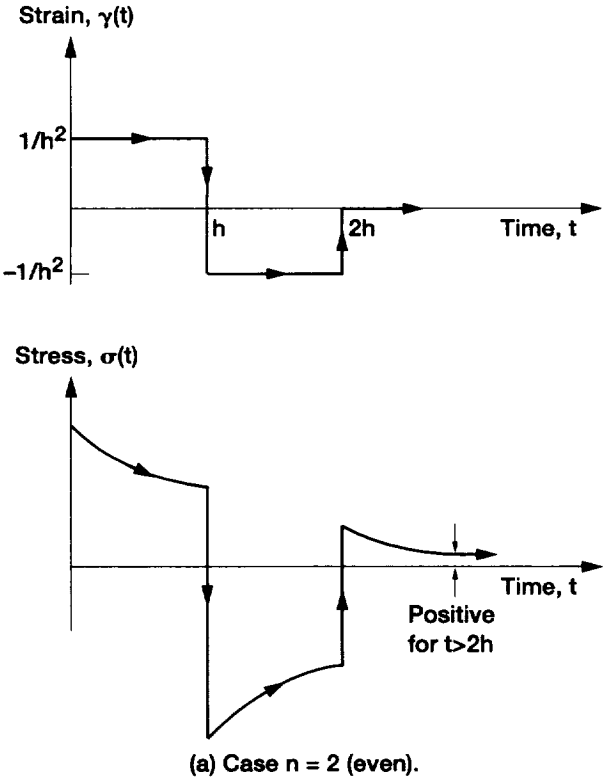

(a) Case n = 2 (even).

Fig 7.—Step-strain loading approximating functions $\gamma^{(n)} = \frac{(-1)^n}{h^n}\sum_{k=o}^{n}(-1)^{n-k}\frac{n!}{k!(n-k)!}\gamma(kh)$ in the limit h→o. According to fading-memory assumption, stress relaxes to positive or negative values for even (Case a, n = 2) or odd (Case b, n = 3) n-th order derivatives.

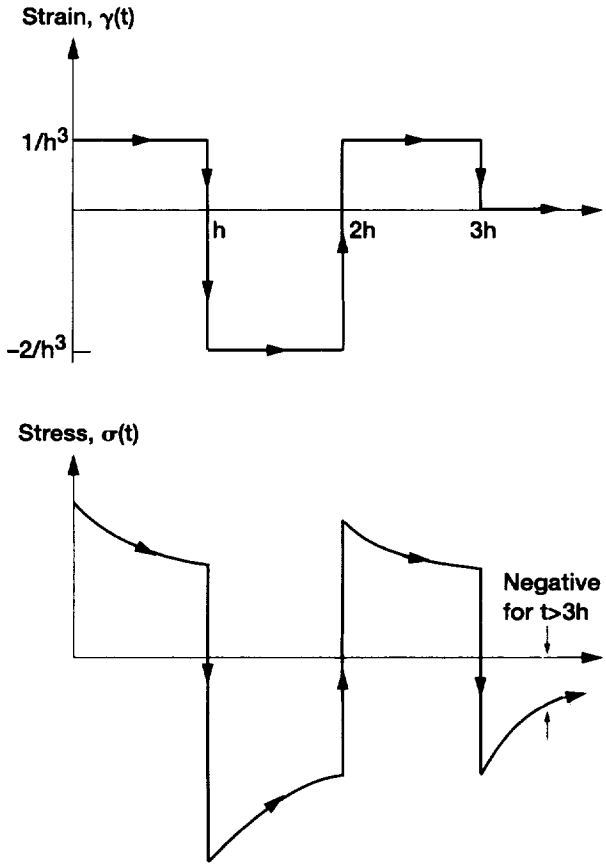

(b) Case n = 3 (odd).

Fig 7.—Concluded.

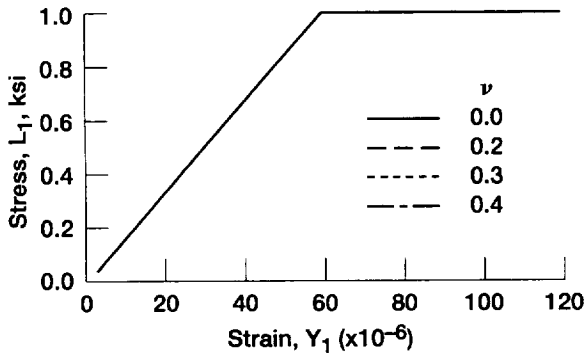

Fig 8.—Stress versus strain histories in the 1 direction given equal Poisson's ratios, see cases 1-4 of Table 1.

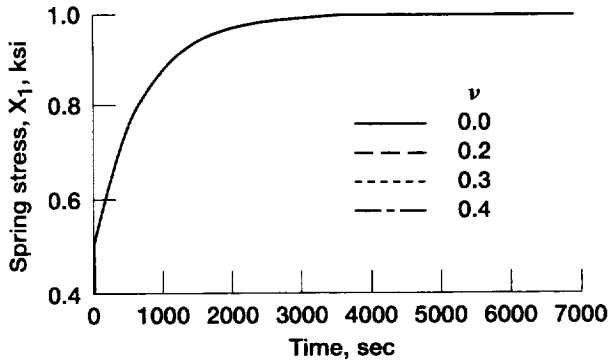

Fig 11.—Equilibrium stress (X) in the 1 direction versus time given equal Poisson's ratios, see cases 1-4 of Table 1.

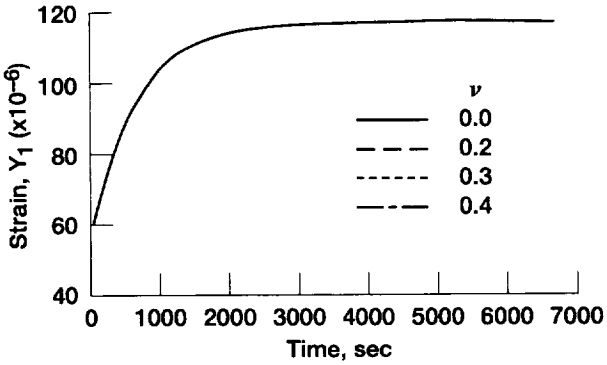

Fig 9.—Total reversible strain in the 1 direction versus time given equal Poisson's ratios, see cases 1-4 of Table 1.

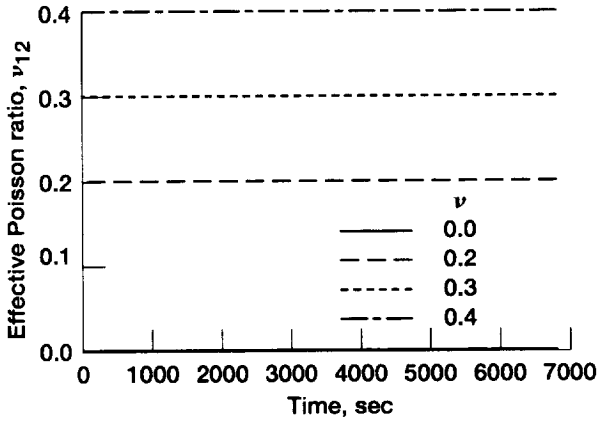

Fig 12.—Effective overall Poisson's ratio versus time given equal Poisson's ratios, see cases 1-4 of Table 1.

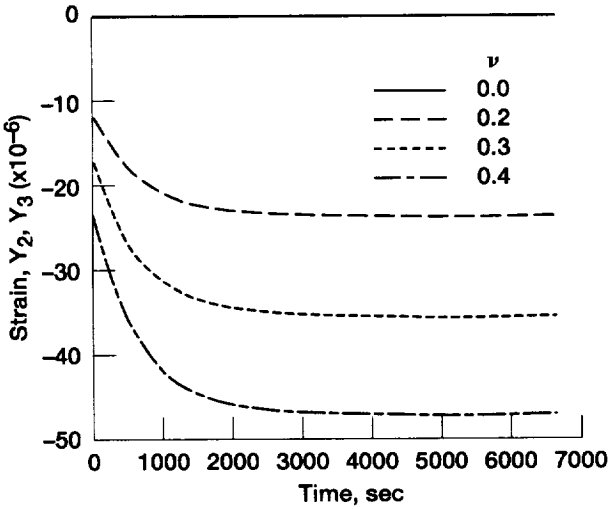

Fig 10.—Total reversible strain in the 2 and 3 direction versus time given equal Poisson's ratios, see cases 1-4 of Table 1.

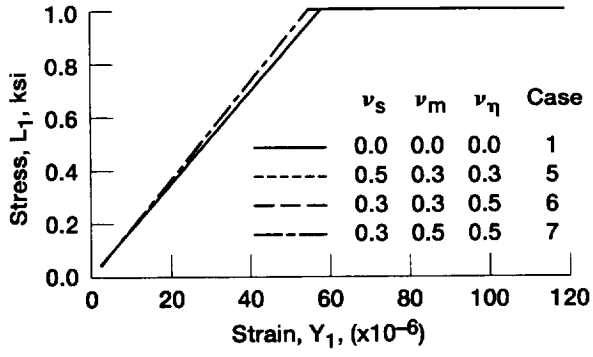

Fig 13.—Applied stress versus strain histories in the 1 direction given nonequal Poisson's ratios, see cases 1, 5, 6 and 7 of Table 1.

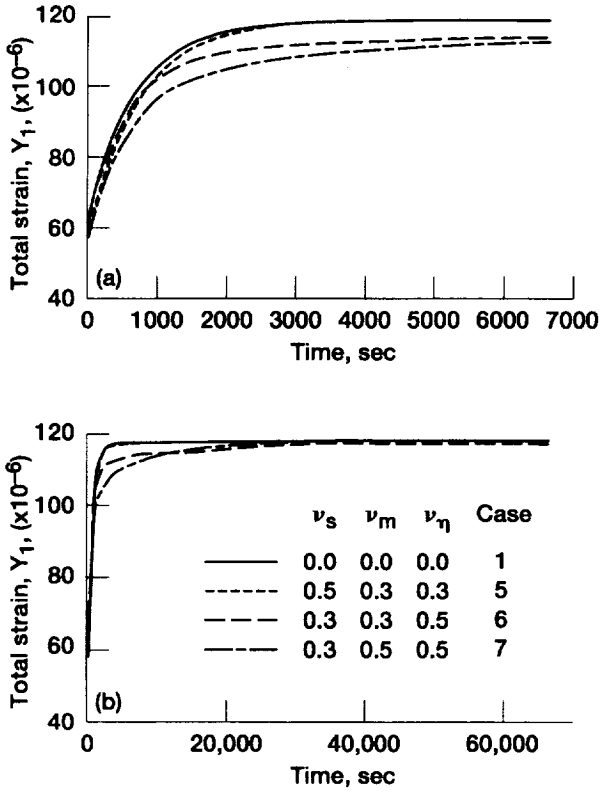

Fig 14.—Total reversible strain in the 1 direction versus time given nonequal Poisson's ratios, see cases 1, 5, 6 and 7 of Table 1. (a) 10 γ. (b) 100 γ.

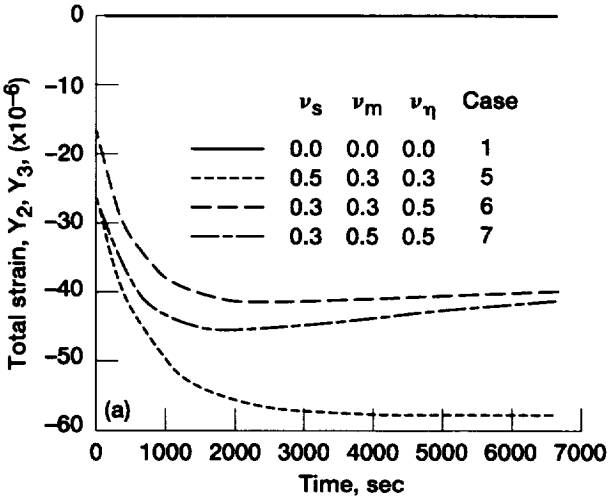

Fig 15.—Total strain in the 2 and 3 directions versus time given nonequal Poisson's ratios, see cases 1, 5, 6 and 7 of Table 1. (a) 10 τ. (b) 100 τ.

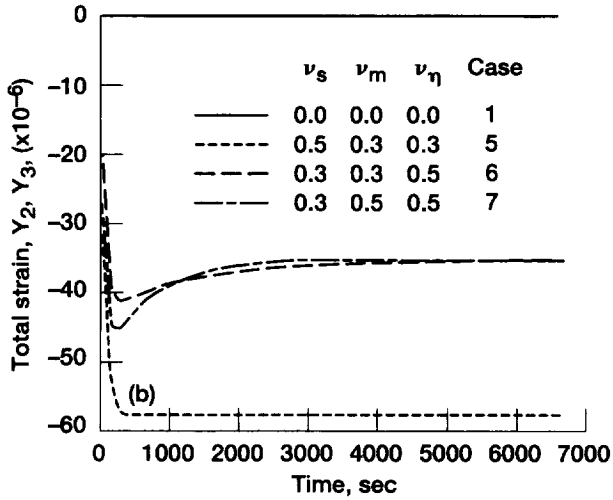

Fig 15.—Concluded. (b) 100 τ.

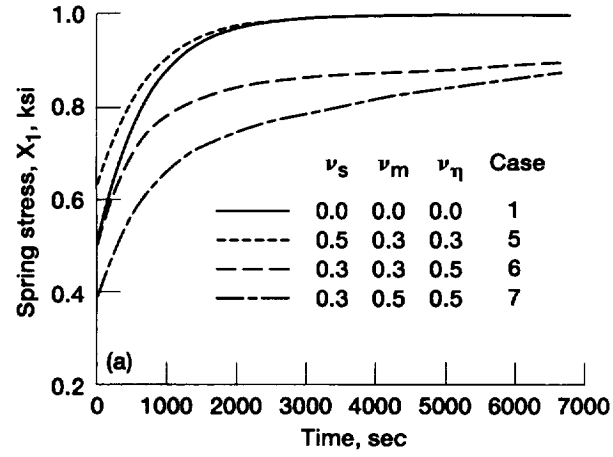

Fig 16.—Equilibrium stress in the 1 direction versus time given nonequal Poisson's ratios, see cases 1, 5, 6 and 7 of Table 1. (a) 10 τ. (b) 100 τ.

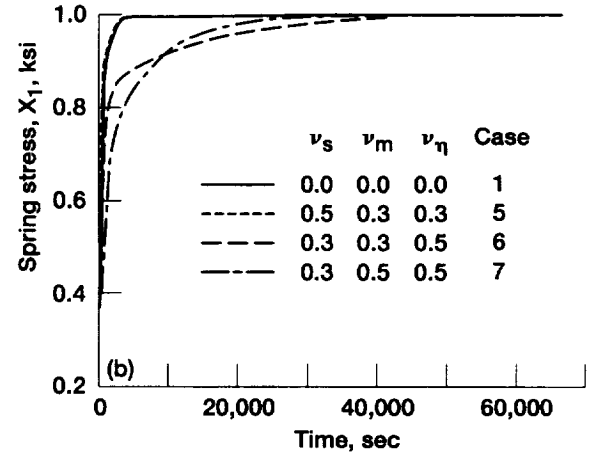

Fig 16.—Concluded. (b) 100 τ.

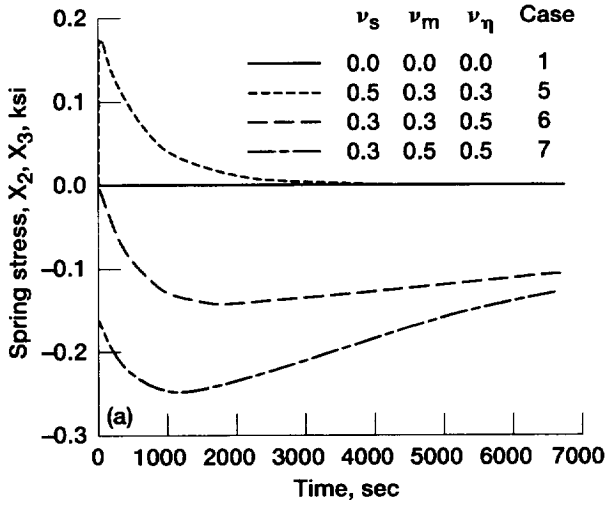

Fig 17.—Equilibrium stress in the 2 and 3 directions versus time given nonequal Poisson's ratios, see cases 1, 5, 6 and 7 of Table 1. (a) 10 τ limit. (b) 100 τ limit.

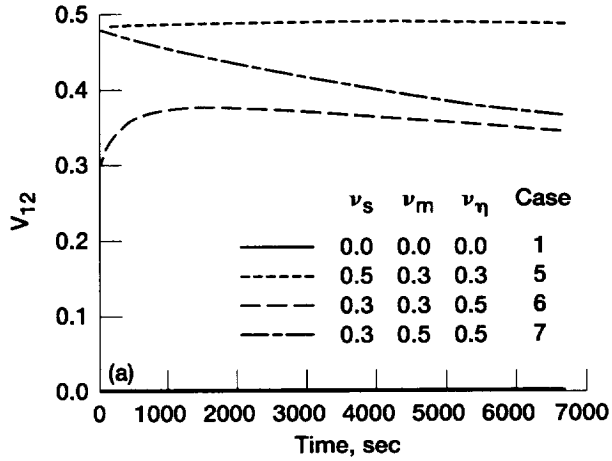

Fig 18.—Effective overall Poisson's ratio (V_{12}) versus time given nonequal Poisson's ratios, see cases 1, 5, 6 and 7 of Table 1. (a) 10 τ limit. (b) 100 τ limit.

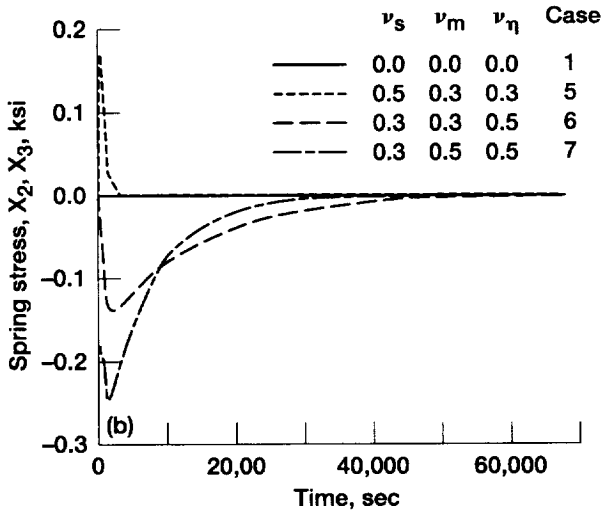

Fig 17.—Concluded. (b) 100 τ limit.

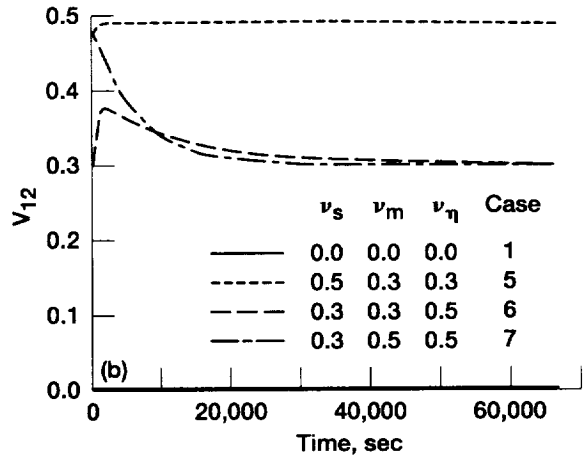

Fig 18.—Concluded. (b) 100 τ limit.

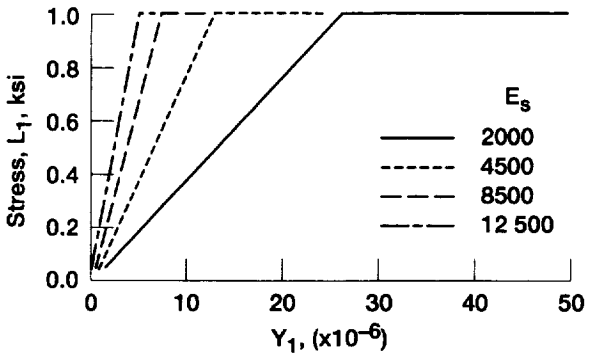

Fig 19.—Influence of E_s on stress (L) versus strain (Y) in the 1 direction, see Table 2.

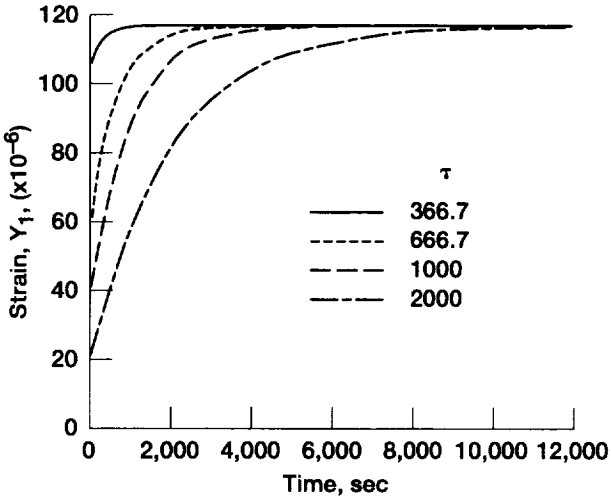

Fig 22.—Influence of τ on total strain (Y) in time response, see Table 3.

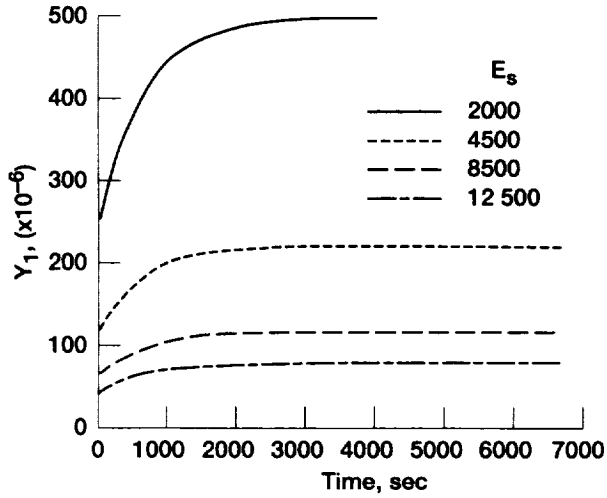

Fig 20.—Influence of E_s on total strain (Y) in the 1 direction verses time, see Table 2.

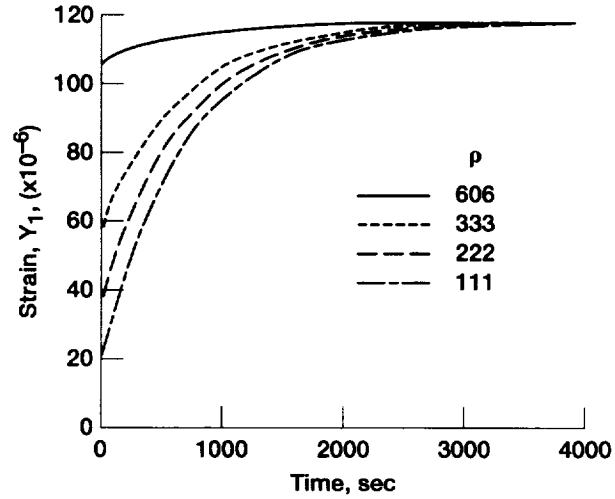

Fig 23.—Influence of ρ on total strain (Y) in time response, see Table 4.

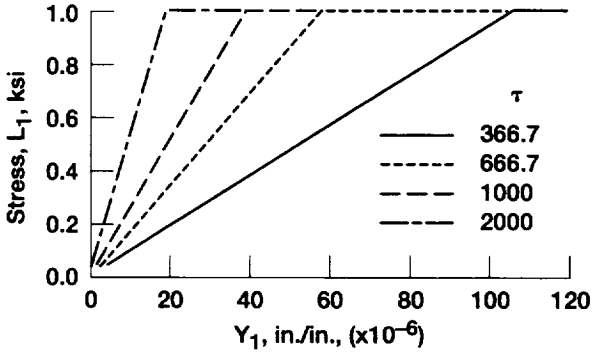

Fig 21.—Influence of τ on stress (L) versus strain (Y) history in the 1 direction, see Table 2.

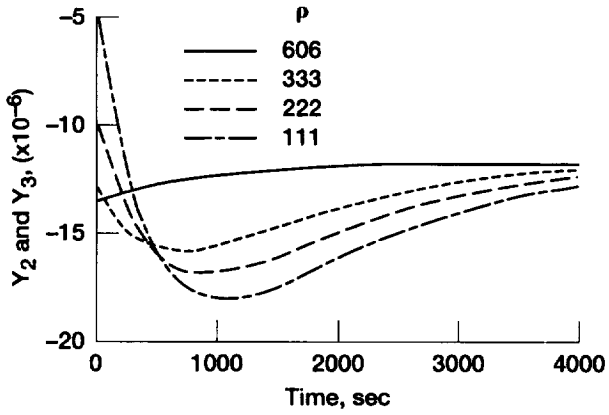

Fig 24.—Influence of ρ on total strain histories in the 2 and 3 directions given different Poisson's ratios in the spring and Maxwell elements.

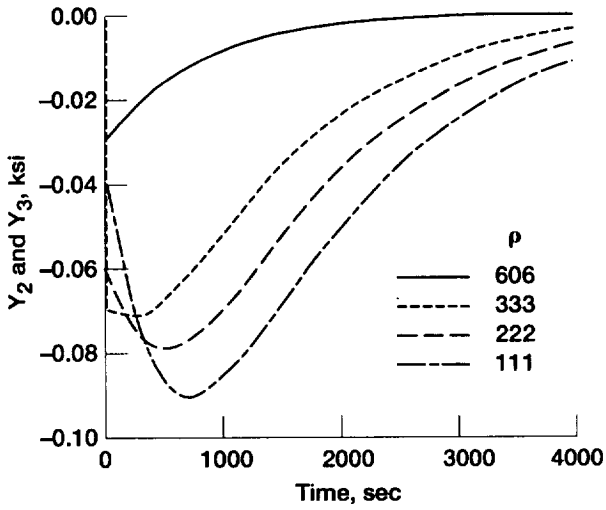

Fig 25.—Influence of ρ on equilibrium stress (X) versus time in the 2 and 3 directions given different Poisson's ratios in the spring and Maxwell elements.

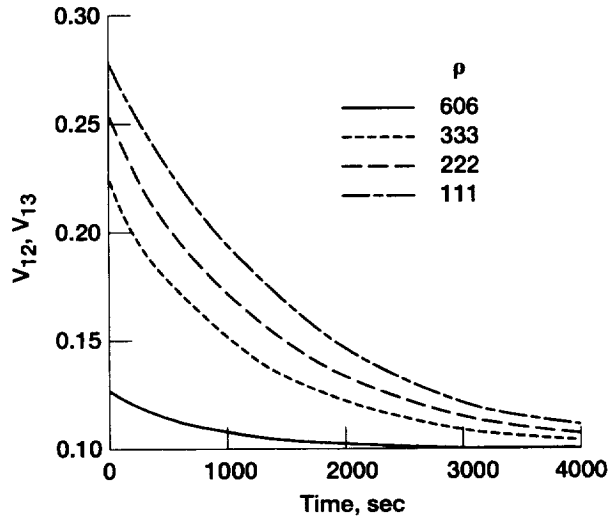

Fig 26.—Influence of ρ, given different Poisson's ratios in the spring and Maxwell elements, on the effective Poisson's ratio (V_{12}) history.

REPORT DOCUMENTATION PAGE

Form Approved
OMB No. 0704-0188

1. AGENCY USE ONLY (*Leave blank*)	2. REPORT DATE	3. REPORT TYPE AND DATES COVERED
	December 1997	Technical Memorandum

4. TITLE AND SUBTITLE

A General Reversible Hereditary Constitutive Model:
Part I–Theoretical Developments

5. FUNDING NUMBERS

WU–523–21–13–00

6. AUTHOR(S)

A.F. Saleeb and S.M. Arnold

7. PERFORMING ORGANIZATION NAME(S) AND ADDRESS(ES)

National Aeronautics and Space Administration
Lewis Research Center
Cleveland, Ohio 44135–3191

8. PERFORMING ORGANIZATION REPORT NUMBER

E–10791

9. SPONSORING/MONITORING AGENCY NAME(S) AND ADDRESS(ES)

National Aeronautics and Space Administration
Washington, DC 20546–0001

10. SPONSORING/MONITORING AGENCY REPORT NUMBER

NASA TM–107493

11. SUPPLEMENTARY NOTES

Responsible person, S.M. Arnold, organization code 5920, (216) 433–3334.

12a. DISTRIBUTION/AVAILABILITY STATEMENT

Unclassified - Unlimited
Subject Category: 39 Distribution: Nonstandard

This publication is available from the NASA Center for AeroSpace Information, (301) 621–0390.

12b. DISTRIBUTION CODE

13. ABSTRACT (*Maximum 200 words*)

Using an internal-variable formalism as a starting point, we describe the viscoelastic extension of a previously-developed viscoplasticity formulation of the complete potential structure type. It is mainly motivated by experimental evidence for the presence of rate/time effects in the so-called quasilinear, reversible, material response range. Several possible generalizations are described, in the general format of hereditary-integral representations for non-equilibrium, stress-type, state variables, both for isotropic as well as anisotropic materials. In particular, thorough discussions are given on the important issues of thermodynamic admissibility requirements for such general descriptions, resulting in a set of explicit mathematical constraints on the associated kernel (relaxation and creep compliance) functions. In addition, a number of explicit, integrated forms are derived, under stress and strain control to facilitate the parametric and qualitative response characteristic studies reported here, as well as to help identify critical factors in the actual experimental characterizations from test data that will be reported in Part II

14. SUBJECT TERMS

Viscoelastic; Hereditary behavior; Nonisothermal; Deformation; Multiaxial; Thermodynamics

15. NUMBER OF PAGES

45

16. PRICE CODE

A03

17. SECURITY CLASSIFICATION OF REPORT	18. SECURITY CLASSIFICATION OF THIS PAGE	19. SECURITY CLASSIFICATION OF ABSTRACT	20. LIMITATION OF ABSTRACT
Unclassified	Unclassified	Unclassified	